Nitrogen doped RGO Supported ZnTe Nanocomposites for Photodegradation of Congo red dye

Yusra Hawa

Regn. #173037

A thesis submitted in partial fulfillment of requirements

for the Degree of MS in

Chemistry

Supervised by: Dr.Muhammad Fahad Ehsan

Department of Chemistry

School Of Natural Sciences (SNS)

Nation University of Sciences and Technology (NUST)

H-12, Islamabad, Pakistan

2018

FORM TH-4

National University of Sciences & Technology

MS THESIS WORK

We hereby recommend that the dissertation prepared under our supervision by: Yusra Hawa, Regn No. 00000173037 Titled: Nitrogen doped RGO Supported ZnTe Nanocomposities for Photodegradation of Congo Red dye be accepted in partial fulfillment of the requirements for the award of **MS** degree.

Examination Committee Members

1. Name: Dr. Muhammad Arfan   Signature:_____

2. Name: Dr. Mudassir iqbal   Signature:_____

External Examiner: Dr. Faroha Liaquat   Signature:_____

Supervisor's Name: Dr. M. Fahad Ehsan   Signature:_____

_____
Head of Department

07/09/18
_____
Date

COUNTERSINGED

Date: 07/09/18

_____
Dean/Principal

THESIS ACCEPTANCE CERTIFICATE

Certified that final copy of MS thesis written by **Ms. Yusra Hawa**, (Registration No. **000001730370**), of **School of Natural Sciences** has been vetted by undersigned, found complete in all respects as per NUST statutes/regulations, is free of plagiarism, errors, and mistakes and is accepted as partial fulfillment for award of MS/M.Phil degree. It is further certified that necessary amendments as pointed out by GEC members and external examiner of the scholar have also been incorporated in the said thesis.

Signature: _____

Name of Supervisor: Dr. M. Fahad Ehsan

Date: _____07/09/18_____

Signature (HoD): _____

Date: _____07/09/18_____

Signature (Dean/Principal): _____

Date: _____07/09/18_____

Dedication

Every inspiring work wants self-determination along with supervision of elders particularly those who are very near to our heart, I humbly dedicate all my achievements that I have made so far, and whatever success I would make in the years to come to

Jasmin

(My Mother)

Her love, prayers, faith and encouragement made me what I am today!

Acknowledgments

Table of Contents

Chapter 1: Introduction

Chapter 2: Literature Review

Abstract

References

Chapter 3: Experimental

Abstract

Chapter 4: Results and Discussion

Abstract

Chapter 5: Summary and Future Prospects

List of Abbreviations

CB	Conduction Band
CR	Congo Red
DRS	Diffuse Reflectance Spectroscopy
EDX	Energy Dispersive X-Ray Spectroscopy
eV	Electron Volt
GO	Graphene Oxide
NRGO	Nitrogen Doped Reduced Graphene Oxide
RGO	Reduced Graphene Oxide
SEM	Scanning Electron Microscopy
VB	Valence Band
XRD	X-Ray Diffraction
XPS	X-Ray Photoelectron Spectroscopy
ZnTe	Zinc Telluride

List of Figures

List of Schemes

List of Tables

Abstract

Various forms of dyes are used in fabric productions and the polluted water is ejected as it is without any treatment for the removal of harmful dyes. Such contaminated water is unsafe for both the human and animal health. Hence, treatment of such polluted water is very necessary. Photocatalyis has proved to be really effective method in converting these contaminated compounds to less toxic compounds *e.g.* H_2O and CO_2. Zinc telluride (ZnTe) is considered as promising semiconductor due to its small band gap and their activity in visible light. Regardless of its interesting properties, ZnTe exhibit fast e^- h^+ recombination rate as a result of which overall photocatalytic activity is affected. In addition, nanocompoistes with varying ZnTe content were synthesized using solid state grinding. The prepared catalysts were analyzed via several characterization techniques including x-ray diffraction (XRD) for the phase confirmation, scanning electron microscopy (SEM) to investigate the surface morphology, electron dispersive x-ray (EDX) for the compositional analysis, x-ray photoelectron spectroscopy (XPS) and UV-Vis diffuse reflectance spectroscopy (DRS) to plot the alignment of energy levels with the help of valence band position and band gap, respectively. All the synthesized samples were used for the degradation of CR dye. High photocatalytic degradation efficiency of ~ 97.6% was observed over the composite with equal amounts of both ZnTe and NRGO, which might be attributed to the reduced charge recombination.

Chapter 1
Introduction

1.1 Nanotechnology:

Nanotechnology has taken giant attention over time. Nanoparticles are the important element of nanotechnology. Nanoparticles are particles having size range among 1 and 100 nanometers. These are composed of organic matter, metal, metal oxides or Carbon. At nanoscale the nanoparticles shows a characteristic chemical, biological, and physical properties which are totally changed from their single atoms, molecules or bulk materials. This is due to high surface area to volume ratio, increased in mechanical strength, high stability or reactivity, spatial confinement etc. and because of these properties nanoparticles are use in different field [1]. Nanoparticles is basically consist of three covers that is **(a)** the external layer, which could be joined with polymers, metal ions, and also with different types of small molecules. **(b)** The second one is the shell layer that is chemically different in all direction from the core shell and **(c)** the layer which is consider as the basic part of nanoparticles and mostly termed the nanoparticles itself, are the core layer [2].

1.2 Nanoparticles Classification:

The nanoparticles are different from other materials, because of its various dimensions, shapes and sizes. The nanoparticles have various structure, size and shapes. It can be tubular, spherical, flat, spiral, conical or irregular. On the basis of dimensions nanoparticles can be a zero dimensional where all the dimension are measured in nanoscale ranged and stable at a distinct point e.g. nano dots. Nanoparticles which contain only one parameter are called one dimensional e.g. graphene, twofold dimensional where it contain two parameter i.e. length and breadth e.g. carbon nano tubes or nanoparticles which contains all the parameters i.e. length, breadth, and height are three dimensional like gold nanoparticles. Nanoparticles can either be amorphous or crystalline in nature with multi or distinct crystal solid [3].On the basis of chemical and physical properties nanoparticles are classified into following types;

1.2.1 Carbon Based Nanoparticles:

Nanoparticles which are completely consist of carbon atom are called carbon based nanoparticles. The two major classes of carbon based nanomaterials are carbon nanotubes and fullerene.

Fullerene:

Fullerene is the allotropic form of carbon which twisted to form the hollow cage of arranged hexagonal and pentagonal units of carbon, each carbon atom exhibits SP^2 hybridization state. Due to its high strength, electron affinity, versatility and electrical conductivity they have generated noteworthy commercial interest.C_{60} and C_{70} are the well know examples of fullerene [4].

Carbon Nanotubes:

The detection of carbon nanotubes disclose a new period in material sciences in 1991.A carbon nanotubes consists of carbon having a tube like shaped. Its diameter lying in nanometer scale, 0.7nm for single layered and 100nm for multilayer carbon nanotubes and length varying from few μm to several mm. Carbon nanotubes exhibit the peculiar behavior due to its strong bonding between their atoms. The metallic or a semiconductor nature of CNT depend how the graphene sheet has rolled up to form the tubes. To control or increased the conductivity of polymer carbon nanotubes are used because it can conduct electricity and heat [4].

1.2.2 Inorganic Nanoparticles:

Metal oxide and metal based nanoparticles are generally placed into this class. Those particles which are not made up of carbon are classified into inorganic nanoparticles.

Metal Nanoparticles:

Nanoparticles that are prepared from metal are metal based nanoparticles. Zinc, cadmium, lead, cobalt, copper and aluminum are the most widely used metals for nanoparticles synthesis. Nanoparticles of gold, copper and silver and alkali metal show a wide absorption band in the visible area of electromagnetic spectrum. These nanoparticles are used in several research fields because of their advanced optical properties. For the

sampling of SEM nanoparticle of gold is widely used for coating as it increases the electron stream that help in gaining high quality images of SEM [5].

Metal Oxide:

Particles that are synthesized to improve the properties of their corresponding metals are metal oxide nanoparticles. To obtain the high reactivity and efficiency these nanoparticles are synthesized, e.g. in the existence of oxygen at normal temperature nanoparticle of iron immediately oxidizes into iron oxide, which shows that the reactivity of iron oxide is high than that of pure nanoparticle of iron. Aluminum oxide, magnetite, silicon dioxide and titanium dioxide are the common example of metal oxide based nanoparticles [5].

1.2.3. Organic Nanoparticles:

Ferritin, micelles and dendrites, etc. are called organic nanoparticles. These nanoparticles are nontoxic, shows high reactivity towards electromagnetic and thermal radiation.
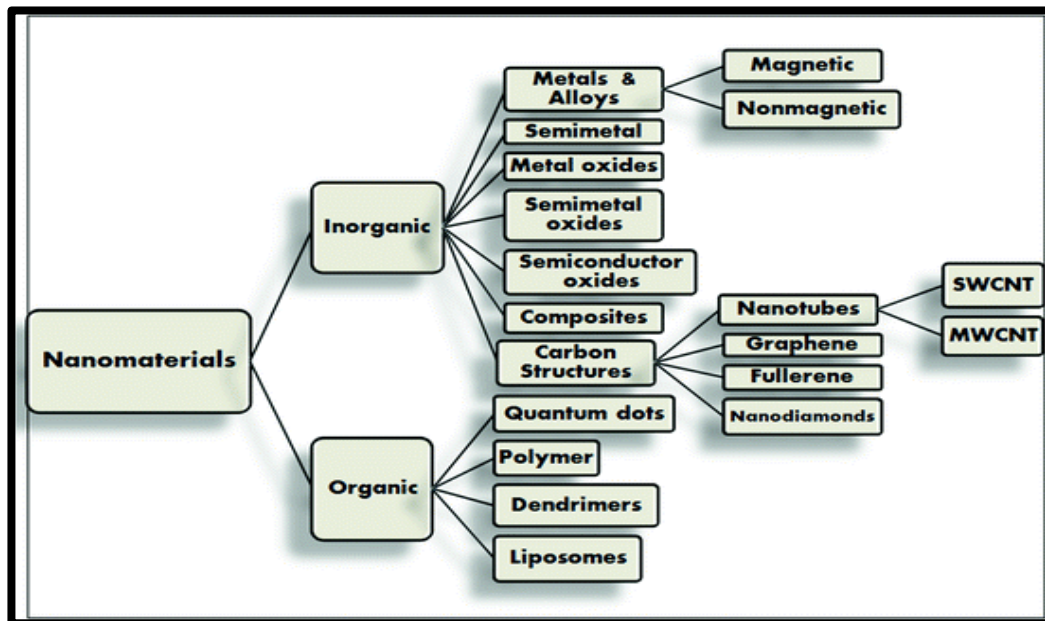
Figure 1.1: Nanomaterials Classification [4]

For drug delivery systems organic nanoparticles are mostly used because of its high efficiency it can be injected on definite part of the physique which is also called targeted

drug delivery [5].These nanoparticles are further classified into four classes that are Dendrimers, Quantum dots, polymers and liposomes.

1.3. Application of Nanoparticles:

Nanoparticles show unique application in different fields because of their unexpected small size, high surface area, physical, chemical and mechanical properties. The most common applications of nanoparticles are given below;

1.3.1. Sunscreen and Cosmetics:

The ordinary ultraviolet protection sun blocker lacks everlasting stability during usage. Nanoparticles of titanium dioxide and zinc oxide use as a sunscreen provide countless advantages, because these nanoparticles are translucent to visible light beside to absorb and reflect the UV light. Nanoparticles of Iron oxide are use in some lipsticks as a pigment [6].Fig 1.2 shows some fascinating applications of nanomaterials.
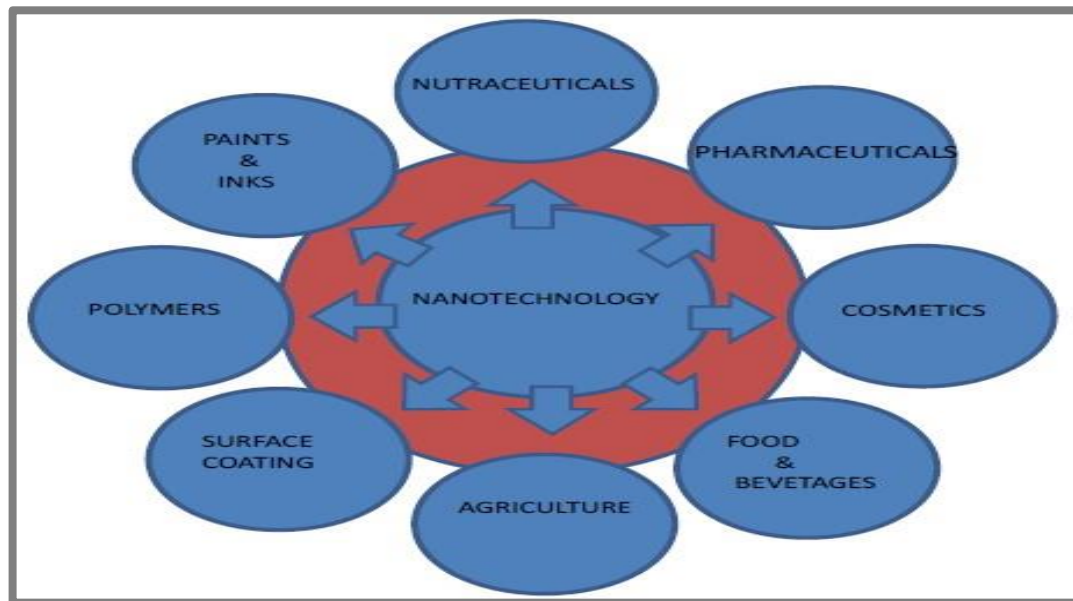
Figure 1.2: Applications of nanoparticles

1.3.2. Medicine:

The use of nanoparticles in drug delivery has upgrade the medical field, using nanoparticles the drug can be transport to the target cells. This procedure reduced the side

effects, the cost, and total drug consumption. Nanotechnology also shows the significant role in the replication and repair of damage tissue. In Ayurveda an Indian medical system, gold is used in many applications. Gold is used in certain medical production for memory enhancement [7].

1.3.3. Electronics:

Nanoparticles also play the important role in display technology e.g. in the LEDs of modern displays nanocrystalline zinc selenide, cadmium sulphide and lead telluride are used. The development in laptop computers and mobile phones required high demand for high capacity and light weight batteries. For separator plate in batteries nanoparticles are used which store more energy as compared to conventional batteries because of their foam like structure. Because of large surface area of nanocrystalline metal hydride and nickel batteries require less recharging and last longer .For the detection of gases like nitrogen dioxide and ammonia nanoparticles are used because of their high electrical conductivity [8].

1.3.4. Construction:

The development of nanotechnology making the construction processes safer, affordable and quicker e.g. mechanical properties and strength of normal concrete is increased by mixing nanosilica and hematite respectively [9]. The properties of steel, which is the most extensively used material in manufacture industry, can be increased by applying nanotechnology e.g. in bridge construction nano size steel is used because of its high strength. The addition of nanoparticles in paints increases the self-healing, Insulation abilities and also its performance by making them lighter [10]. Thus when used e.g. on airplane, it might decrease their total mass and the amount of paint necessary, that is favorable to the atmosphere.

1.3.5 Nanoparticles and Environment:

Nanoparticles has become an ideal choice now days to be used in environmental remediation due to its distinct physical and chemical behavior .Nano remediation has played important rule in treatment of water, air and soil. Main mechanism involving in purification is redox reactions. Nanoparticles are used for decontamination of surface water, municipal and industrial waste water.Conventional chemical methods are replaced

by nanoparticles due to its low cost, lower quantity and higher efficiency. Soil contamination is also treated by injecting nanoparticles into specific target areas [11].

1.4 Environmental Pollution:

Pollution is the introduction of foreign substance, toxic contaminant or any form of energy, (light and noise) into the environment that causes sewer damage to earth. One of the greatest problems facing today by world is an environmental pollution that is increasing with every passing year and causing irreversible and serious damage to earth. Different types of pollution based on the area of environment affected are given below:-

- **Water pollution**
- **Soil pollution**
- **Radioactive pollution**
- **Noise pollution**
- **Thermal pollution**
- **Air pollution**
- **Light pollution**

Approximately two thirds of earth is enclosed by water and remaining part is covered by land. Non availability of clean water and sanitation is one of the most glaring problems faced by people now a day in the world. This problem is further aggravated as fresh water reservoirs are depleting day by day [12].Water pollution is basically the pollution of water bodies like ground water, lakes and rivers etc. It occurs when the contaminants are directly or incidentally enters into water bodies without suitable treatment to eliminate the harmful compounds. Water pollution is not only damaging the plants and organisms existing in these water bodies but also damaging the natural occurring societies. Not only the industrial effluents but also some natural processes, like earth quakes,storms,and algae blooms are also disturbing the value of water The major causes of water pollution are:-

- Industrial Discharge
- Use of Excessive Pesticides
- Domestic Waste
- Excessive Pharmaceutical Products

6

- Organic Compounds (Dyes, Dioxin and PCBs)

1.5 Dyes:

A dye is a colored material which has attraction for a particular substance to which it is applied. Like dyes pigments are also colored substances because both absorb wavelength of visible light. But the main difference between pigments and dyes lying in their solubility dyes are soluble in water while pigments are insoluble in water. Dyes color is due to:-

- Its absorption of light in the visible area of spectrum at a certain wavelength.
- Containment of chromophores,these are the compound which give color
- Aromatic in nature.
- Exhibit conjugations[13]

Dyes, aromatic in nature are used in the form of aqueous solution and it is easily soluble in water due to the presence of auxochromes group that is $-NO_2$, $-NHR$, $-NH_2$, $-OH$, $-Br$,$-Cl$, $COOH$ [63] etc.

1.5.1 Classification of Dyes:

There are several ways of classification of dyes. Dyes may be classified on the basis of its synthesis, nature of chromophore, use of source material and nature of the electronic excitation [14-15].General classification of dyes is shown in given fig;
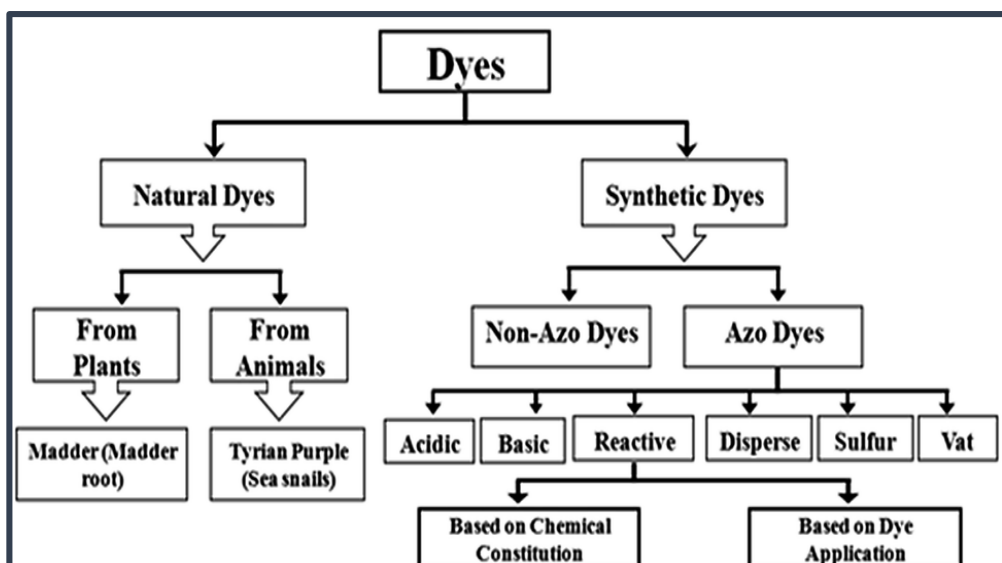
Fig 1.3: Classification of dyes

Natural and synthetic dyes are the two main types of dyes. Natural dyes are derived from plants, minerals and animals e.g. madder dye and red dyes are extracted from madder root and kamala tree while tyrian purple and red violet dyes are extracted from snail and lac insect respectively. Mauveine, was the first synthetic organic dye, discovered by William Henry Perk in 1856.A synthetic dyes are formerly derived from coal tar derivatives but now a days these dyes are prepared from benzene and its derivatives. On the basis of nature, synthetic dyes are further classified in to azo dyes and non azo dyes. Azo dyes can be acidic, basic, disperse, sulphur, vat and reactive in nature.

1.5.2 Toxic Effect of Dye and Decolourization Techniques:

Dyes plays important role in our day to day life. They are used in various industries, including cosmetics, textiles, leather, paints and plastics however dyes when discharged from industries causes serious water pollution due to its stable nature as it does not decomposes easily. For wet processing of textiles large volumes of water and chemicals are consume by textile industries. These chemical reagent may be organic, inorganic or polymer in nature. The incidence of very little concentration of dyes in wastes is extremely undesirable and visible. Out of **7×10^5 tons** annual production of dyestuff in the world, 10-15 % is wasted in water during its synthesis and application process [16]. Some toxic effect of dyes are given below

- Dyes effect photosynthetic activity of underwater plants by decreasing the absorption and reflection of sun light, diminishes the soil quality and disturbs the plant growth
- Due to presence of metals and aromatics compounds, these dyes have toxic effect on aquatic e.g. dyes containing heavy metal damage the gills of fishes and human life.
- Dyes have teratogenic, mutagenic and carcinogenic properties.

To address these issues there is a dire need to carry out research to find out ways for water purification [17]. Following methods are used for removal of dyes

- **Physical Methods:**

Physical method involved the removal of substances with the help of naturally occurring forces like Vander walls forces, gravity, by use of physical barriers and electrical

8

attraction. Membrane filtration, coagulation, irradiation, adsorption by activated carbon and ion exchange are examples of physical methods. Although these are economically feasible, but produces large amount of sludge.

- **Biological Methods:**

Biological method detached the dissolved organics from waste consequently reduces the biological and chemical oxygen demands of the effluents. Different microbes are used for adsorption of dyes like white rot fungi, which convert the dissolved and colloidal carbonaceous organic compound into several gases. Large volumes of dyes, that are soluble in water, can be removed through this method at low cost but this method is not suitable for treatment of all types of dyes because certain dyes have affinity for these microbes.

- **Chemical Methods:**

In this method various chemicals are used to expedite disinfection. It is also used along with physical and biological cleaning processes to attain various water standards. Chemical methods include oxidation process, ozonation, sodium hypochlorite, fentons reagent and photochemical treatment.

Although all the above techniques have been used are found fairly effective to reduce the toxic effect of dyes from industrial waste water but the main problem of these methods are production of secondary pollutant which cannot be dumped and treated again as such.

1.6 Photocatalysis:

Photo catalysis is special class of oxidation technique known as advanced oxidation process that is characterized by production of hydroxyl radical. Photo catalysis is derived from two words photo means light and catalysis, a process that increases rate of reaction with the help of catalyst. Catalyst is a substance that increases rate of reaction by decreasing minimum energy required for chemical reaction. Thus photo catalysis is process which uses light to activate that substance which is used for modification of chemical reaction and the substance which modifies the rate of chemical reaction by using light is called photocatalyst. In the presence of water and light photocatalyst generates electronic holes and strong oxidation reagents to breakdown the organic compound in to water and carbon dioxide. Plant chlorophyll is a typical example of natural photocatalyst.

It is an advance process of nano chemistry and due to its increasing demand; scientist's interest in this field is increasing day by day [18].

1.6.1 Characteristics of Photocatalyst:

Different semiconductor are used as photo catalyst like cadmium sulphide, zinc oxide, titania, zinc selenide etc. Following should be the characteristics of an ideal photocatalyst:-

- Stable in sunlight
- Readily available
- Chemically unreactive
- Ability to captivate the reactant
- Large surface area
- Adsorption potential
- Small size

Quantum size affects the properties of nanomaterials therefore by varying the semiconductor particle dimension; it is possible to increase the redox potential of the electrons in conduction band and holes in valence band.

1.6.2 Steps Involved in Photocatalysis:

Following are the main steps involved in photocatalysis [19]:-

- Light absorption and generation of electron and hole pairs
- Oxidation of donors species
- Reduction of acceptor
- Electron hole pair recombination

Reduction and oxidation are two basic steps involved in application of photocatalyst

1.6.3 Factors Affecting Photocatalytic Degradation:

The efficacy of photocatalytic system is greatly dependent on various operative factors that direct the photodegradation of pollutant. Some of the important factors which effect the photodegradation ability of photocatalyst are given below;

- Influence of Dye concentration

- Influence of Ph
- Amount of catalyst
- Surface area
- Structure and size of catalyst
- Inorganic ions
- Reaction Temperature
- irradiation time and light intensity

The photocatalysis process depends on dye, that are adsorbed on the surface of photocatalyst because in such procedure only the dye adsorbed on the external of catalyst contribute and not one in bulk of solution. Mostly degradation efficiency of photocatalyst falls by enhancing the concentration of dye using constant amount of photocatalyst. The photodegradation of dye enhances with increasing the ratio of catalyst because as the catalyst amount increases more active sites become available on the surface of photocatalyst hence causing an increase in creation of hydroxyl radical which can participate in degradation of dye solution. Increase in reaction temperature also increases the photocatalytic activity however temperature above 80 °C causes the recombination of electrons and holes hence reduces the activity. Deactivation of photocatalyst and reduction in efficiency of photon can be occur, when the high concentration of pollutant are used. At low intensities of light the activity enhances as intensity of light increases however at transitional intensity of light the rate is depend on the square root of light intensity. But when the intensity of light increases the photo generated electron and hole pairs compete with recombination as result producing lower effect on the reaction rate. For a good photocatalytic activity Ph of medium should be optimum, Studies reveal that at lower Ph titania show maximum absorption, results in high photocatalytic activity [20].

1.7 Graphene:

Graphene is the two dimensional monoatomic thick allotrope of carbon atom packed in honey comb like structure and has SP^2 carbon atom packed in a single sheet. Andre Geim and Kostya Novoselo for the first time isolated graphene in 2004 by using top down approach [21].One atom thick layer of graphite known as graphene can be folded to get one dimensional carbon nanotubes, can form three dimensional graphite by stacking and

its rapping give the zero dimensional fullerenes. It has distinct mechanical, optical and electrical properties. Carbon atoms contain six electron out of which four electron are present in valence shell which is utilized in chemical bond formation. But in case of graphene out of four three electrons form strong bond with the neighboring atoms resulting in sigma bond formation while the remaining one electron in each carbon atom form pi bond with the neighboring atoms consequential in the creation of highly conjugated structure which is highly conductive in nature. Graphene is considered one of the strongest materials due to its high value of Young's modulus and spring constant. Graphene has high heat conductivity and large surface area that is 2630 $m^2.g^{-1}$ according to theoretical calculation. Highly conjugated structure and large surface area allow graphene to adsorb other conjugated compound through pi-pi interaction. [22-25].

1.7.1 Routes for Synthesis of Graphene:

There are large number of procedures, used for synthesis of graphene depending on the nature of starting material, yield of product and technique followed. Broadly methods used for synthesis of graphene are classified into top-down technique, involved the exfoliation of graphite or its derivative like graphite fluoride and graphene oxide into modified graphene or graphene sheet. This method is widely used for application of polymer composites. Second one is the bottom up approach where graphene is synthesized through various methods including reduction of graphene oxide, micromechanical exfoliation, arc-discharge, chemical vapor deposition and epitaxial growth [26].

1.7.1.1 Chemical Vapor Deposition:

It is a type of bottom –up approach, where various precursor compounds are placed in the reaction chamber. These precursor molecules get deposited on the pre heated substrate after mixing in the reaction chamber. In thermal CVD suitable substrate are used which have the ability to high carbon solubility. The substrate is then placed in CVD chamber having temperature 1000⁰C and vacuum pressure 10^{-3} Torr, where carbon is diffuse into the substrate at growth temperature followed by the rapid quenching of the substrate. Graphene is produced after precipitation of diffuse carbon. The wideness of graphene layers depend on the rate of cooling and diffused quantity of carbon [27].

1.7.1.2 Mechanical Exfoliation:

Another method used for synthesis of graphene is mechanical exfoliation, where graphene is exfoliated by using both organic and aqueous solvents with or without surfactant using for stabilizing the exfoliated sheet. N-methyl pyrrolidone is considered the most suitable solvent for mechanical exfoliation because of its high yield and high dispersion. Although monolayer unoxidized graphene is produce but high boiling point and expensive nature of solvent make this process uneconomical and difficult [14].High quality and single layer graphene can be synthesized without using any solvent by flaking highly oriented pyrolytic graphite available commercially through scotch tape. Mechanical exfoliation produces graphene in high quality without producing any kind of defects which is not comparable with other method, the reason is this process occur at normal temperature, no strong reagent and vigours condition are required [28-30].

1.7.1.3 Unzipping of Carbon Nanotubes:

In this method high argon plasma is passed through polymer embedded narrow walled carbon nanotubes which scrapes the side wall faster than rest opening CNTs Into GPRs, nanoribbons planar graphene followed by removal and deposition of polymer over substrate [31-32]

1.7.1.4 from Different Precursor:

By using different precursor like 10,100-dibromo-9, 90-bianthryl graphene can be synthesized. In this method thermal deposition of monomer take place and as a result two radical species are produce per molecule by removing halogens from precursor molecules. Through cyclohydrogenation these radical species add to each other yielding highly conjugated network [28].

1.8 Graphene Oxide:

Graphene oxide is generally composed of pseudo two dimensional carbon layers synthesized through Staudenmeier, Hummers, and Hofmann. Depending on the nature of graphite precursor, synthesis technique and reaction condition oxidation level may vary. These methods are different from each other on the nature of acids and oxidizing agent used during graphene synthesis. Staudenmeier method uses potassium per chlorate and fuming nitric acid, sodium nitrate and potassium per manganate uses in Hummers method

and Hofmann method involves using concentrated nitric acid along with potassium per chlorate [33-34].
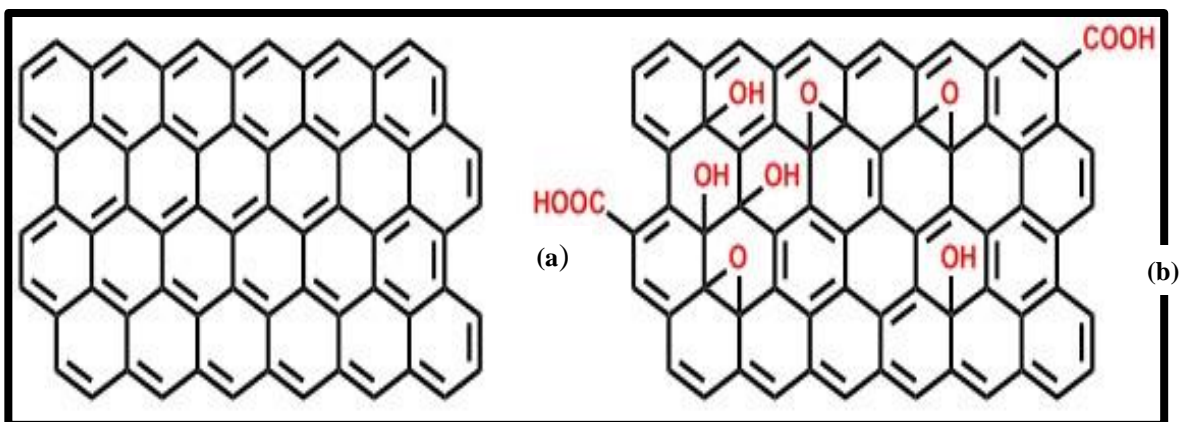
Fig 1.4: Structure of (a) graphene (b) graphene oxide [35]

Graphene oxide contains different polar groups like hydroxyl, epoxide and carboxylate attached with each carbon sheet in aliphatic six membrane structure. The hydroxyl and epoxide group are located at the upper and lower sheet of graphene while at the edge of graphene sheet carboxylic group is located. These function group presence at the basal and edge, convert the SP^2 network of graphene into SP^2 and SP^3 frame work. The SP^3 defects cause the distortion of pi conjugated system as a result lowering its conductivity and strength. Also this functional group strongly disturbs the chemical and electrical properties of graphene oxide therefore making the properties of graphene different from graphene oxide. Although the presence of these functional group made the graphene oxide hydrophilic in nature and easily isolated in water but its presence causes barrier in their electrical conductivity making them unfavorable to use in electronics [35-36].Through ultra-sonication or thermal shock GO can be separated into 2D nanosheets.

1.9 Reduce Graphene Oxide:

Graphene oxide is nonconductive in nature due to the existence of oxygen functionalities and SP3 defects. Generally reduction is done to restore the conjugated framework and to remove the oxygen functionalities. Different methods are used for this process including electrochemical, thermal and chemical. During reduction process firstly the hydroxyl and epoxy group presence at the basal plane of graphene oxide are removed while carboxylic group and ester located at the edge does not affect the conductive behavior of graphene

oxide readily. Secondly defects can be healed by doping the graphene using carbon monoxide or nitrogen oxide or through CVD of carbon using ethylene. Major steps involved during synthesis of reduced graphene oxide are shown in given scheme.
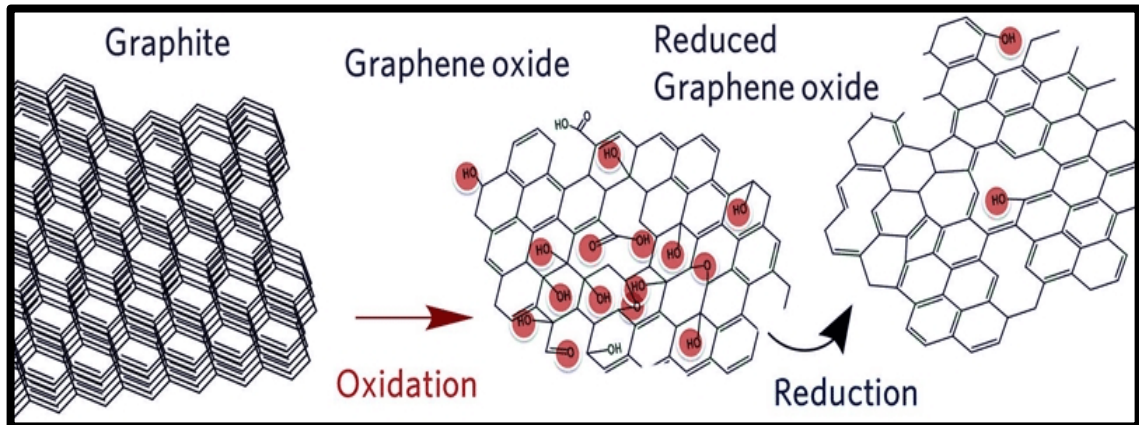
Scheme 1: Steps involved during synthesis of reduced graphene oxide [39]

Electrical conductivity of graphene oxide is increased after removal of functional group and healing defects opening way towards the numerous field e.g. conductive inks [37] electronic sensor fabrication [38], energy storage etc., all governed by the charge transfer and electronic structure of the sheet.

1.10 Method of Synthesis for Nanocomposite:

Different methods are used for synthesis of nano composites based on the needs of different properties and morphologies. Each method has its own benefits and drawbacks, some method are best for nano particles synthesis while some were found to be more efficient for synthesis of specific morphologies like nano tubes, nano sheets, nano wires etc.[40-41]].Common method being used for synthesis of nano composite are appended below:-

- Sono chemical method
- Sol-gel method
- Chemical vapor deposition
- Micro wave method

- Hydro thermal and solvo thermal method

1.10.1 Sono Chemical Method:

It is a type of chemical reaction which uses ultra-sonic waves.Acoustaic cavitation is the main phenomenon that produces sononchemical effect in solutions. Cavitation is basically the production, growth and then collapse of bubbles in liquid as a result high pressure, intense heating and liquid jets steams are produced. In this method ultrasonic bath is used where a solution of metal oxide and solvent is stirred for two hours under normal temperature. The resulting solution is then transferred to ultrasonic bath where this solution is irradiated with ultra-sonic waves for specific temperature and time. The obtained solution is then centrifuged and dried at a specific temperature to obtain the desired material .Although this method is used for obtaining the narrow size and pure samples but the availability of large scale ultra-sonic reactor makes less reliable [42]

Scheme 2: Synthesis of Sn-C-dots nanoparticle via sono-chemical method [42]

1.10.2 Chemical Vapor Deposition Method:

In this method solution in the vapor state are condensed to get a solid phase material. This method is widely used for coating on different material, which is done for obtaining good

16

thermal, mechanical, electrical and optical properties. To start the deposition process thermal energy is used which heat the gas in gas chamber [43]

1.10.3 Sol-Gel Method:

It is a method in which the colloidal liquid (Sol) is converted into a semi solid (Gel) form. In this process particles from a colloidal suspension are settled into a pre-existing surface resulting in a ceramic material. Stable dispersion of colloidal polymers or particles in the solvent is a Sol. These particles are either crystalline or amorphous in nature. Particles in a gaseous phase are Aerosol while particles in a liquid phase are called Sol. A gel is a three dimensional continuous network that enfolds a liquid phase. Polymer gel contains particles having polymeric sub-structure while in colloidal gel the particles are made of accumulation of colloidal particles. The Sol particles interact with each other through Hydrogen bonding or Vander walls forces.
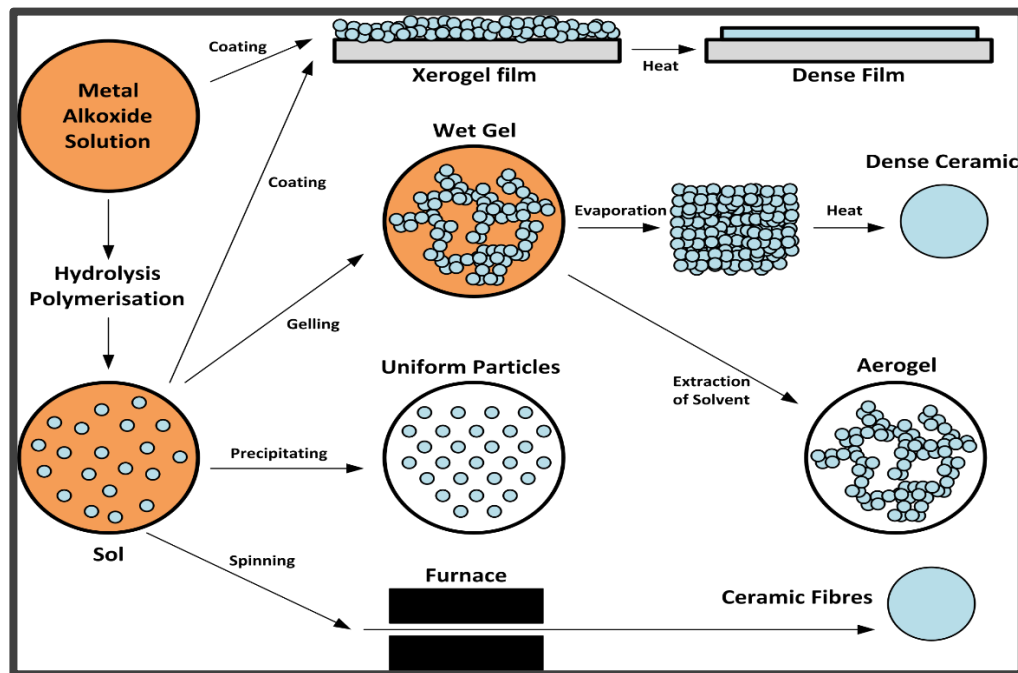
Fig 1.5: Illustration of Sol Gel method

This process is used for the formation of integrated network that is gel from colloidal particle or chemical solution [sol].Hydrolysis and polycondensation of precursors occurs

17

resulting into colloid formation. Precursors used for this process are metal chlorides or metal alkoides.The sol is slowly converted towards liquid like phase gel. Metal hydroxo or metal axo polymers are generated by connecting metal centers with hydroxo or axo bridges. After drying process, from the gel liquid phase is removed. To increase mechanical properties and for polycondensation it is further treated thermally through calcination [44].

1.10.4 Microwave Method:

This is a very neat and simple method in which electromagnetic radiations of low energy and high frequency (900 - 2450 MHz) are used to synthesize nano-structure materials [45].

1.10.5 Hydrothermal and Solvothermal Method:

It is a heterogeneous chemical synthesis that is carried out in a closed system called autoclave under highly optimum conditions (temperature higher than 100C and pressure above 1 atm) in the presence of water as solvent. In this process a suitable solution is placed in autoclave and it is sealed, the container is then placed in an oven at a high temp and pressure. The sample obtained is then filtered, washed and annealed at suitable temperature to gain the nano structure in fine powdered form [46]. The autoclave is made of steel and has Teflon lining. This method is widely used for synthesis of smaller particles in ceramic industries. It is also used for synthesis of nano tubes, nano wires and nano rads. This process is overall best reported. The main difference between hydrothermal and solvothermal method is the solvent that is used. It is used mainly for the synthesis of nano particles [47].

1.11 Characterization Technique:

After the synthesis of nanomaterial, next steps involved are the analysis of surface morphology, optical properties, phase purity, crystallite size and elemental composition. For this, different methods are used; including Transmission and Scanning Electron Microscope, UV-Visible Spectroscopy, Powder X-ray Diffractometry, IR Spectroscopy and Electron Spin Resonance Spectroscopy.

1.11.1 X-Ray Diffraction:
Basic Principle

XRD is an analytical technique used for both qualitative and quantitative analysis. In order to find the crystal structure, phase composition, defects, unit cell parameters, grain size and Barvais lattice this method is used.

Mechanism

In this method, a beam of a specific wave length (X-ray) is thrown on the crystal surface at a certain angle. The beam is reflected back by the atomic planes as the rays interact with the electrons of atoms. The atomic planes of the crystal structure have a semi-transparent nature so it allows a part of the X-ray to pass through it and reflect the other part. X-ray diffraction is based on principle of constructive interference of incident beam and sample. It will occur only when the conditions meet Bragg's law. Bragg's law is the relationship of interplanar distance of atoms, angle of incident beam and wavelength.

For constructive interference, path length of two rays is equal to whole number of wavelength.

$$N\lambda = 2d\sin\theta$$

Where **d** is inter planner distance, λ is wavelength of X-rays, θ is Incident angle, **n=1** for monochromatic beam

Scherer's formula is used for the determination of particle size of crystallites that is;

$$D = K\lambda / B\cos\theta$$

Where, **D** is particle size of crystallites, **K**=0.9, λ is wavelength of X-rays, B is full width half maxima and θ is the Bragg angle in degrees

Diffractometer consist of following parts;

- sample and sample holder
- incident beam optics
- cathode X-ray tube
- detector and goniometer

The X-ray generated from cathode tube are directed on to the sample. The strength of reflected X-ray is noted through detector. The detector then converts the signals and

transmits it to the monitor of computer. To maintain the angle and rotation of a sample, goniometer is used.
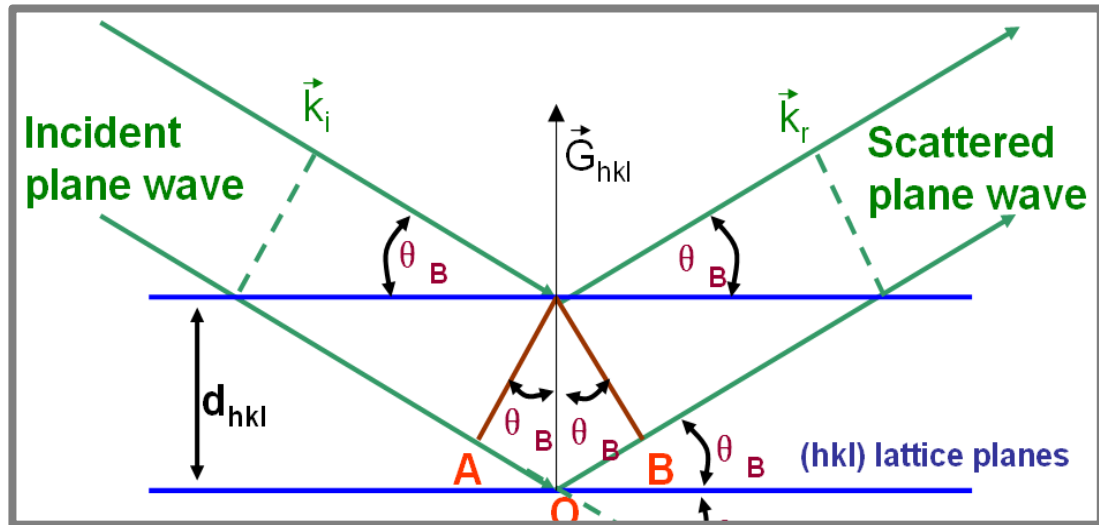
Figure 1.6: Bragg's law of diffraction

1.11.2 Scanning Electron Microscopy:

Basic Principle

It is one of the important methods which is very useful to judge the morphology, elemental composition and topography of a sample.

Mechanism:

It is a kind of electron microscope where an intensive beam of electrons are scanned over a surface of a sample to get an image. Scanning electron microscope consist of following components

- Electronic filament
- Column with electromagnetic lenses
- Sample chamber
- Computer hardware and software

In this process electrons are produced from electron gun and passed down in a column through apertures and different lenses to generate a focused beam of electrons. Electron beam strike the surface of a sample and this interaction can be of two types. **Elastic**

collision in which the energy is conserved and back scattered electrons are produced. Second one is **inelastic collision** in which energy is transferred to sample and secondary electrons are produced**.** Then electron beams scan the surface of sample with the help of scan coils. Electron sample interaction results in production of signals which are than detected by a detector.
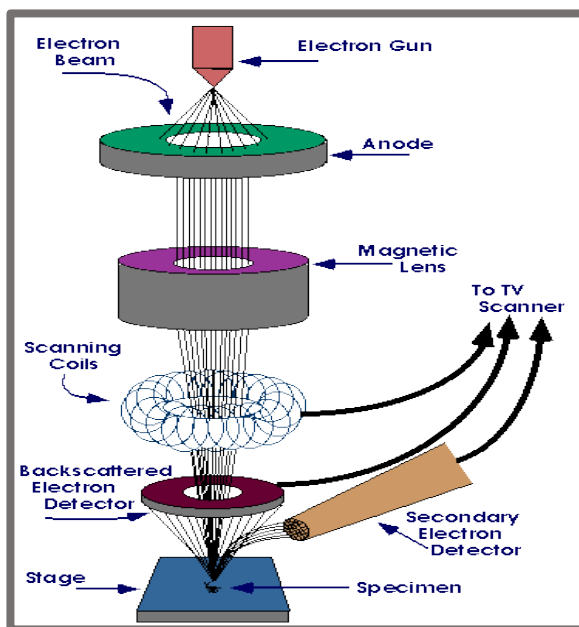
Figure 1.7: Representation of scanning electron microscopy

1.11.3 UV-Visible Spectroscopy/DRS Analysis:

Basic Principle:

Absorption spectroscopy is working on the principle of absorption of light by the material. The material absorbs the photon only when the energy of light is equal or greater than the energy difference between the two states. The excitation of electron from low energy level to the high energy states and then relaxation from the high energy to lower energy state give information about the electronic structure.

Mechanism:

UV-Vis spectroscopy is used for both qualitative and quantitative analysis of sample. The region 200-800nm corresponds to visible region of the spectrum whereas ultra violet region is from 200-380nm.when UV-Vis radiation is absorbed by the molecule electrons are excited from HOMO to LUMO.Energy difference between the HOMO and the LUMO

are designated as band gape energy.UV-Vis analysis follows Beer- Lambert law, According to this law "when a ray of monochromatic light passes over the solution there is decreased in the intensity of incident light which is directly proportional to the concentration of solution.

$$A = \epsilon c l$$

Where, A=absorbance

l=path length in cm

ϵ=molar absorptivity

c=concentration of solution in ML^-1.

We can calculate the absorbance of solution by keeping the path length constant. The graph between absorbance on X-axis and wavelength on Y-axis is designated as UV-Vis spectra. We can find out the band gap of the prepared catalyst from this graph by constructing the tauc plot. Firstly the plot between photon energy (hv) versus $(\alpha hv)^{1/2}$ is constructed. An extrapolation of a line at particular region in the graph touches the x-axis at a specific value which indicates the value of band gap for a particular semiconductor.

Following are the main components of UV-Vis spectrophotometer;

Light Source:

Halogen and Deuterium lamp are used as a source of light in UV-Vis Spectrophotometer. Halogen lamp provides radiation in visible region while Deuterium lamp is used for ultra violet region.

Monochromator:

Monochromator is a device used for isolating a narrow portion of a spectrum. It is used to breakdown the light rays into single wavelength through this we can extracted the desired wavelength.

Sample Stage:

Spectrophotometer can be used for the detection of liquid, solid and gases form of samples but for liquids sample we use a special type of container made of glass or silica known as cuvette**.**
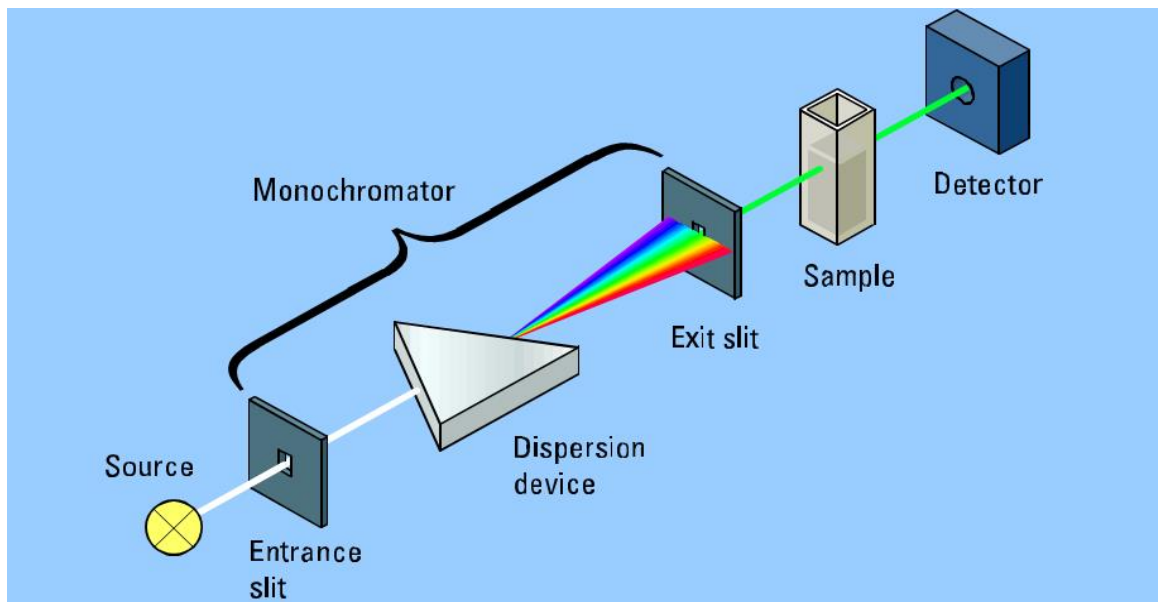
Figure 1.8: Representation of UV-vis spectroscopy

Beam Splitter:

Beam splitter is used to split the beam originating from light source. In single beam spectrophotometer single light beam from source moves to detector. While in double beam the light splits into two beams after passing through the monochrometr one for the reference and one for the sample. Due to fast and non-tedious working, and wide scanning range double beam spectrophotometer is widely used as compared to single beam spectrophotometer.

Detectors:

Charge couple device, photodiode are used as a detector in spectrophotometer. Beam of light after being passed through the sample is sent to the detector where its intensity is measured against its wavelength.

1.11.4 Diffuse Reflectance Spectroscopy:

DRS is an optical method which is commonly used to describe the electronic behavior present in the structure of materials in solid form. DRS and UV-Visible spectroscopy are closely related to each other. In both techniques, visible light is used to cause excitation of electron from VB to CB. But in UV-Visible spectroscopy, the relative change in transmittance of light is measured however in DRS the relative change in reflectance of light is measured as it passes over sample. Kubelka-Munk transformation is used to manipulate the reflectance data into tauc plot.

1.11.5 Energy Dispersive X-ray Spectroscopy:

Basic Principle

Its characterization ability is based on the principle that each element has a distinctive atomic structure that permits X-rays that are representative of an element's atomic structure for identification.

Mechanism:

When a beam of light is fall on a surface of sample electrons are excited from the inner shell as a results of which holes are created after its ejection from inner shell. To fill that vacant space electrons from higher energy level fall down as a result X-rays are emitted. X-ray fluorescence spectrometer is used as a detector in EDX. The detectors detect the X-rays which is then sent to analyzer which plots the relative abundance of the X-rays against their energy to obtain its spectra. Every element has its own characteristic spectra so this technique can be used to characterize elements by the spectra by EDX.Components of EDX include:

- Source of X-ray
- Pulse processor
- Electrostatic and magnetic sector
- Detector
- Analyzer
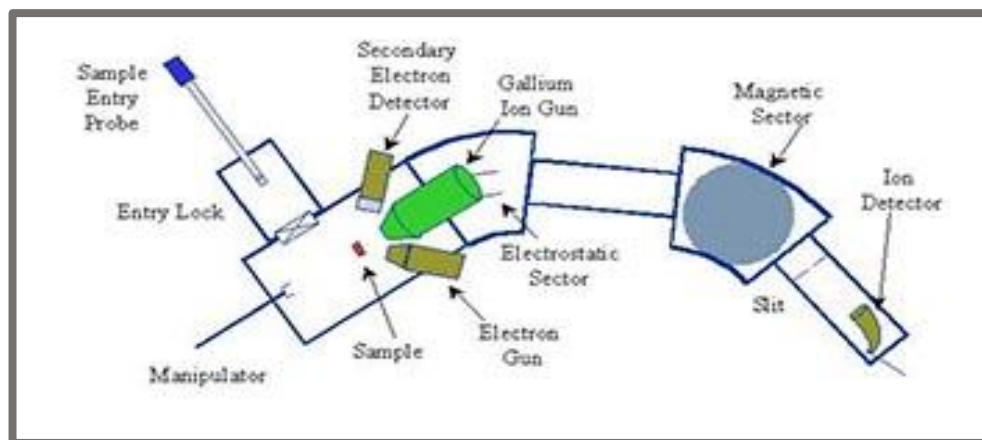
Figure 1.9: Representation of EDX

1.11.6 X-Ray Photoelectron Spectroscopy:

XPS is used to investigate the surface chemistry of a sample. Electronic and chemical states of elements, elemental composition and empirical formula can be analyzed through XPS.X-rays is fall on the surface of sample and its kinetic energy is measured. The electrons emitted from 1-10nm surface of the sample are analyzed. The plot between the ejected electrons and their Kinetic energies give a photoelectron spectrum. Each atom eject the electrons of specific energy and results in formation of peaks. Elements present on the surface of the material can be identified through the intensity and energy of the peak. XPS consist of following components:

- X-rays Source
- An ultra-high vacuum
- Energy analyzer
- Magnetic field shielding
- Electron detector
- Analyzer

A monoenergetic beam of X-ray is used to eject the photoelectron from the surface of a sample. X-rays of different energies either Ka (1486.6ev) or $MgKa$(1253.6ev) are used. To increase the mean free path of photons, ions and electrons, Remove the adsorbed gases and excessive contamination from the sample surface ultra-high vacuum is employed. Kinetic energy of emitted electron can be measured through analyzer. The binding

25

energies can be measured through the peak position and element present in the sample identified.

1.12 Objective and Structure of this Work:

This thesis explains the synthesis of zinc telluride and N-doped RGO through hydrothermal method and graphene oxide by Hummers method. The objective of thesis was to make the nanocomposites that can be easily used for degradation of dyes. Following are the detailed objective of this thesis

- Synthesis of ZnTe by hydrothermal method
- Synthesis of graphene oxide sheet by Hummers method
- Incorporation of Nitrogen atom into graphene to increase the transfer rate of electron
- Synthesis of nano composite of ZnTe-NRGO to decrease the e/h recombination rate in ZnTe and to make more efficient against pollutant degradation
- Characterization of Prepared catalyst
- Choosing the best catalyst by performing degradation studies of Congo red

References:

[1]. Hasan, Saba and Idrees. "A review on nanoparticles: their synthesis and types." *Research Journal of Recent Sciences* 2277 (2015): 2502.

[2]. Balbus, John M., John M., Andrew D., Maynard and Vicki L., Colvin. "Hazard assessment for nanoparticles." *Environmental Health Perspectives* 115.11 (2007): 1654.

[3]. Shin, Won-Kyung, Jinhyun Cho, Aravindaraj G. Kannan, Yoon-Sung Lee, and Dong-Won. "Cross-linked composite gel polymer electrolyte using mesoporous methacrylate-functionalized SiO_2 nanoparticles for lithium-ion polymer batteries." *Scientific Reports* 6 (2016): 26332.

[4]. Ealia, S. Anu Mary, and M. P. Saravanakumar. "A review on the classification, characterization, synthesis of nanoparticles and their application." *Materials Science and Engineering* (2017): 32019.

[5]. Astefanei, Alina, Oscar Núñez, and Maria Teresa Galceran. "Characterization and determination of fullerenes." *Analytica Chimica Acta* 882 (2015): 1-21.

[6]. Khan, Ibrahim, Khalid Saeed, and Idrees Khan. "Nanoparticles: Properties, applications and toxicities." *Arabian Journal of Chemistry* (2017).

[7]. Shinde, Nishikant C., Nisha J. Keskar, and Prashant D. Argade. "Nanoparticles advances in drug delivery systems." *Res. J. Pharm. Biol. Chem. Sci* 3 (2012): 922-929.

[8]. Liu, Xianghong, un Zhang, Liwei Wang, Taili Yang, Xianzhi Guo, Shihua Wu, and Shurong Wang. "3D hierarchically porous ZnO structures and their functionalization by Au nanoparticles for gas sensors." *Journal of Materials Chemistry* 21.2 (2011): 349-356.

[9]. Nazari, Ali, and Shadi Riahi. "The effects of SiO_2 nanoparticles on physical and mechanical properties of high strength compacting concrete." *Composites Part B: Engineering* 42.3 (2011): 570-578.

[10]. Machado, S., G. Pacheco, H. P. Nouws, Tomas Albergaria, and Cristina Delerue-Matos. "Characterization of green zero-valent iron nanoparticles produced with tree leaf extracts." *Science of the Total Environment* 533 (2015): 76-81.

[11]. Liu, Wen and Taso. "Nanoparticles and their biological and environmental applications." *Journal of Bioscience and Bioengineering* 102.1 (2006): 1-7.

[12]. Forgacs, Esther, Tibor Cserhati, and Gyula Oros. "Removal of synthetic dyes from wastewaters." *Environment International* 30.7 (2004): 953-971.

[13]. Pauling and Linus. "A Theory of the Color of Dyes." *Proceedings of the National Academy of Sciences* 25.11 (1939): 577-582

[14].Gregory and P. Tomas. "Classification of dyes." *The Chemistry and Application of Dyes* (1990).

[15]. Chequer, Farah Maria, Drumond, Gisele Augusto Rodrigues de Oliveira, Elisa Raquel Anastácio Ferraz and Juliano Carballo. "Textile dyes: dyeing process and environmental impact." *Eco-Friendly Textile Dyeing and Finishing*, (2013).

[16]. Xu, Xiang-Rong, Hua-Bin Li, Wen-Hua Wang, and Ji-Dong Gua. "Degradation of dyes in aqueous solutions by the Fenton process." *Chemosphere* 57.7 (2004): 595-600.

[17]. Konstantinou, Ioannis K., and Triantafyllos A. Albanis. "TiO_2-assisted photocatalytic degradation of azo dyes in aqueous solution." *Applied Catalysis B: Environmental* 49.1 (2004): 1-14.

[18]. Khan, Mohammad Mansoob, Syed Farooq Adil, and Abdullah Al-Mayouf. "Metal oxides as photocatalysts." *Applied Catalysis B: Environmental* (2015): 462-464.

[19]. Linsebigler, Amy L., Guangquan Lu, and John T. Yates Jr. "Photocatalysis on TiO_2 surfaces: principles, mechanisms, and selected results." *Chemical Reviews* 95.3 (1995): 735-758.

[20]. Kumar, A., and G. Pandey. "A review on the factors affecting the photocatalytic degradation of hazardous materials." *Material Science and Engineering* 1.3 (2017): 10018.

[21]. Murali, Raghunath, and James D. Meindl. "What is graphene?" *ACM SIGDA Newsletter* 39.8 (2009): 14-23.

[22]. Lee, Changgu, Xiaoding Wei, Jeffrey W. Kysar, and James Hone. "Measurement of the elastic properties and intrinsic strength of monolayer graphene." *Science* 321.5887 (2008): 385-388.

[23]. Chen, Jian-Hao, Chaun Jang, Shudong Xiao, Masa Ishigami, and Michael S. Fuhrer. "Intrinsic and extrinsic performance limits of graphene devices on SiO_2." *Nature Nanotechnology* 3.4 (2008): 206.

[24]. Kuzmenko, A. B., Erik Van Heumen, Fabrizio Carbone, and Dirk Van Der Marel. "Universal optical conductance of graphite." *Physical Review Letters* 100.11 (2008): 117401.

[25]. Ghosh, Suchismita, Wenzhong Bao, Denis L. Nika, Samia Subrina, Evghenii P. Pokatilov, and Alexander A. Blandon. "Dimensional crossover of thermal transport in few-layer graphene." *Nature Materials* 9.7 (2010): 555.

[26]. Berger, Claire, Zhimin Song, Xuebin Li, Xiaosong Wu, Nate Brown and Didier Mayou."Electronic confinement and coherence in patterned epitaxial graphene." *Science* 312.5777 (2006): 1191-1196.

[27]. Kim, Keun Soo, Yue Zhao, Houk Jang, Sang Yoon Lee, Jong Min Kim, Kwang S. Kim, Jong-Hyun Ahn and Philip Kim."Large-scale pattern growth of graphene films for stretchable transparent electrodes." *Nature* 457.7230 (2009): 706.

[28]. Morozov, S. V., Andre K. Geim, Sergei V. Morozov and D. A. Jiang. "Electric field effect in atomically thin carbon films." *Science* 5696 (2004): 666-669

[29].Yang, Xiaoyin, Xi Dou, Ali Rouhanipour, Linjie Zhi and Hans Joachim Räder. "Two-dimensional graphene nanoribbons." *Journal of the American Chemical Society* 130.13 (2008): 4216-4217.

[30]. Jiao, Liying, Li Zhang, Xinran Wang, Georgi Diankov, and Hongjie Dai. "Narrow graphene nanoribbons from carbon nanotubes." *Nature* 458.7240 (2009): 877.

[31].Cain, Jinming, Pascal Ruffieux, Rached Jaafar, Marco Bieri, Thomas Braun and Stephan. "Atomically precise bottom-up fabrication of graphene nanoribbons." *Nature* 466.7305 (2010): 470.

[32]. Hummers Jr, William S., and Richard E. Offeman. "Preparation of graphitic oxide." *Journal of the American Chemical Society* 80.6 (1958): 1339-1339.

[33]. Jalilov, Almaz S., Chenhao Zhang, Errol LG Samuel, William KA Sikkema, Gang Wu and Vladimir Berka. "Mechanistic study of the conversion of superoxide to oxygen and hydrogen peroxide in carbon nanoparticles." *Applied Materials and Interfaces* 8.24 (2016): 15086-15092.

[34]. Staudenmaier, Ber.Deutsch, Georgi Diankov, and Hongjie Dai. "Method for the preparation of graphitic acid." *European Journal of Inorganic Chemistry* 32.2 (1899): 1394-1399.

[35]. Dave, Shreya H., Chuncheng Gong, Alex W. Robertson, Jamie H. Warner, and Jeffrey C. Grossman. "Chemistry and structure of graphene oxide via direct imaging." *ACS Nano* 10.8 (2016): 7515-7522.

[36]. Suk, Ji Won, Richard D. Piner, Jinho, and Rodney S. Ruoff. "Mechanical properties of monolayer graphene oxide." *ACS Nano* 4.11 (2010): 6557-6564.

[37]. Dua, Vineet, Sumedh P. Surwade, Srikanth Ammu, Srikanth Rao Agnihotra, Sujit Jain and K. Roberts. "All-organic vapor sensor using inkjet-printed reduced graphene oxide." *Angewandte Chemie* 122.12 (2010): 2200-2203.

[38]. Bo, Zheng, Xiaorui Shuai, Shun Mao, Huachao Yang and Jiajing Qian. "Green preparation of reduced graphene oxide for sensing and energy storage applications." *Scientific Reports* (2014): 4684.

[39].Shao, Guilin, Yonggen Lu, Fangfang Wu, Changling Yang and Fanlong Zeng. "Graphene oxide the mechanisms of oxidation and exfoliation." *Journal of Materials Science* 47.10 (2012): 4400-4409

[40]. Malekshahi Byranvand, M., A. Nemati Kharat, L. Fatholahi, and Z. Malekshahi. "A review on synthesis of nano-TiO_2 via different methods." *Journal of Nanostructures* 3.1 (2013): 1-9.

[41]. Gaolien, Min-Rui, Yun-Fei Xu, Jun Jiang, and Shu-Hong Yu. "Nanostructured metal chalcogenides: synthesis, modification, and applications in energy conversion and storage devices." *Chemical Society Reviews* 42.7 (2013): 2986-3017.

[42]. Kumar, Vijay Bhooshan, Jialing Tang and Kay Jangweon Lee. "In situ sonochemical synthesis of luminescent Sn/C-dots and a hybrid Sn/C-dots-Sn anode for lithium-ion batteries." *RSC Advances* 6.70 (2016): 66256-66265.

[43]. Swihart and Mark T. "Vapor-phase synthesis of nanoparticles." *Current Opinion in Colloid and Interface Science* 8.1 (2003): 127-133.

[44]. Jones and Ronald William. "Fundamental Principles of Sol--Gel Technology." *The Institute of Metals* 10.1 (1990): 128-137

[45]. Gerbec, Jeffrey A., Donny Magana, Aaron Washington, and Geoffrey F. Strouse. "Microwave-enhanced reaction rates for nanoparticle synthesis." *Journal of the American Chemical Society* 127.45 (2005): 15791-15800.

[46]. Sun, Xiaohong, Chunming Zheng, Fuxiang Zhang, Yali Yang and Guangjun Wu."Size controlled synthesis of magnetite (Fe_3O_4) nanoparticles coated with glucose and gluconic acid from a single Fe^{+3} precursor by a sucrose bifunctional hydrothermal method." *The Journal of Physical Chemistry* 113.36 (2009): 16002-16008.

[47]. Li, Bin, Yi Xie, Jiaxing Huang, and Yitai Qia. "Synthesis by a solvothermal route and characterization of $CuInSe_2$ nanowhiskers and nanoparticles." *Advanced Materials* 11.17 (1999): 1456-1459.

[48]. Koch and Klaus R. "Oxidation by Mn_2O_7: An impressive demonstration of the powerful oxidizing property of di-manganese heptaoxide." *Journal of Chemical Education* 59.11 (1982):973

[49]. Gaul and Wei. "The chemistry of graphene oxide. *"Springer Cham* 8.24 (2015): 61-95.

Chapter 2
Literature Review

Abstract:

This chapter contains reports in literature that was reviewed during this thesis work. There are a lot of research been done on the synthesis of zinc telluride and N-doped reduced graphene oxide, its doping, its nanocomposites synthesis and its activity towards degradation of different kinds of dyes. This chapter also explains the brief mechanism of photocatalysis and also some factors that improve the efficiency of nanomaterial for photocatalyst.

2.1 Photocatalysis:

Photocatalysis is a process where catalyst shows catalytic activity in presence of light. Catalyst become excited upon irradiation of light only, when the photon energy equal or greater than the band gap energy of semiconductor. In photocatalysis the ability of photo catalyst is measured in term of electrons holes pair generation which in turn produced free radical, which are capable to start secondary reaction. When light fall on surface of semiconductor it causes the excitation of e⁻ from conduction band to valance band. After excitation electron holes are generated which are responsible for degradation of organic pollutant. The probable mechanism of photocatalysis is given below [1];

$$Catalyst + hv \rightarrow h^+ + e^-$$

$$h^+ + water \rightarrow \dot{O}H + H^+$$

$$e^- + O_2 \rightarrow O_2^- \cdot$$

$$Pollutant + \dot{O}H \rightarrow CO_2 + H_2O$$

$$\dot{O}H + O_2^- \rightarrow O_2 + H_2O_2$$

$$Pollutant + O_2^- \rightarrow H_2O + CO_2$$

$$Pollutant + \dot{O}OH \rightarrow H_2O + CO_2$$
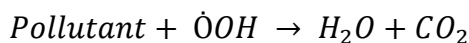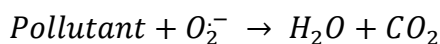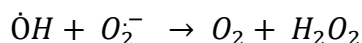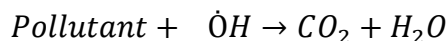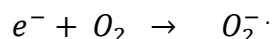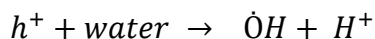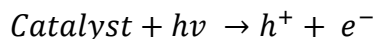
2.2. Electronic Process in Photocatalysis:

Electronic process occurring in photo catalysis is divide into molecular excitation and semiconductor electronic excitation.

2.2.1 Molecular Electronic Excitation:

In molecular electronic excitation firstly highly reactive electronic species are produced through absorption of photon by molecule. Second molecular excitation and excitation event occurs like intersystem crossing, fluorescence, phosphorescence and internal conversion [2-3]

2.2.2 Semiconductor Electronic Excitation

Semiconductor electronic excitation involves;

- Band gap photo excitation
- Band edge position

2.2.2.1 Band gap Photo Excitation:

Semiconductor contain void energy system, where energy levels are not present to favor the recombination of e^- and h^+, produce as a result of absorption of light by solid. Void energy region between the lowest vacant CB and upper filled VB is called band gap. After excitation through the band gap enough life time in ns is available for e^- - h^+ pair to go through charge transfer to adsorbed species, from solution. When semiconductor stays intact and charge transfer is continues the method is called heterogeneous photocatalysis. In this procedure first electron hole pair generated via photon absorption on excitation this photo induced electron and holes can follow different path way. In charge transfer process electron are transfer to electron acceptor for reduction and holes are transfer to surface where e^- from donor species united with hole for oxidation of donor species. The rate of charge transfer process depends upon the redox potential levels of adsorbate and respective position of band edge for valence and conduction band. Recombination of electrons and holes are also in competition with charge transfer process to adsorbate species. Recombination of e^- and h^+ either occur on the surface or in the bulk of semiconductor material. Efficiency of any photocatalyst can be determined through electron-hole recombination rate. In order to decrease the electro-hole recombination rate

various strategies are adopted to increase the photo catalytic activities which are discussed in section 2.3.

2.2.2.2 Band Edge Position:

Band edge position is another parameter that determines photocatalytic activity of semiconductor. Redox potential of adsorbate and band edge location determines the capability of semiconductor. Potential of acceptor species would be more positive as compared to conduction band of semiconductor and potential level of donor species required to be more negative than valance band position of semiconductor that allow the transfer of electron to vacant hole.

2.3 Surface Modification:

Surface modification can be done through doping, coupling one semiconductor with another semiconductor or via addition of metals. Photocatalytic activity of semiconductor depends on stability of semiconductor, wavelength range response and efficiency of photo catalytic process. For example some semiconductor has small band gap and are active in visible range of spectrum but they are unstable and degrade in light with the passage of time like CdS .While some semiconductor has good stability but due to large band gap show poor photocatalytic activity like titania [3].Such limitation can be overcome by modifying surface of semiconductors which leads to following three advantages

*   Increasing the charge separation by decreasing charge recombination rate thus increases photocatalytic activity
*   Enhancing wavelength response range of semiconductor
*   Changing the yield of specific product

2.3.1 Metal Semiconductor Modification:

The addition of metals to semiconductor enhances enhances photocatalytic activity by changing their surface properties. Several studies have done on doping of metals to semiconductors.Sato et al described that photocatalytic activity of titania can be improved by doping with Pt metal. Platinum modifies the properties of titania by changing distribution of electrons. When Pt and titania comes in contact, their fermi level aligns and electron flows to metals from semiconductors, thus electron density decreases in

semiconductors and hydroxyl group acidity increases, thus affecting photocatalytic process on semiconductor surface.

Sclafania, et al. reported the Silver doped titania system. He observed the increased production of Hydrogen from alcohol with Silver doped Titania system. This was credited to trapping of e⁻s on metal site, they observed that the photocatalytic rate of hydrogen production from Silver doped titania is less than Platinum doped titania system. Transmission electron micrograph showed that platinum particle size remains same over 0.5 – 10% platinum on titania. Maximum photocatalytic activity observed with optimum platinum content. Above optimum metal content the efficiency decreases thus the morphology does not determine the efficiency of photo catalyst [4].

2.3.2 Composite Semiconductors:

Combining one semiconductor with other provides another way to increase the charge separation and energy range on the specific system and hence increasing the photocatalytic activity. Gopidas et al reported the synthesis of cadmium sulphide Titania nano composite and observed high photocatalytic activity towards the reduction of Methyl Viologen. TEM images of the CdS/TiO2 photocatalyst confirmed the geometrical interface among several cadmium sulphide particles and with the surface of titania particle. The energy of excitation light is sufficient to stimulate electrons from valence band to conduction band of cadmium sulphide while it is not enough to excite electrons of titania portion of photocatalyst. As the conduction band of CdS is more negative than conduction band of titania. Thus photogenerated electrons from conduction band of cadmium sulphide will transfer to conduction band of titania, thus increasing charge separation and efficiency of photocatalytic process [5]

2.3.3 Surface Sensitization:

Semiconductor having large band gap and visible light inactive can be made visible light active by dye sensitization. Various dyes like erythrosine B, analogues of Ru (bpy) and thionine are used as surface sensitizers. Excitation of an e⁻s from dye to conduction band of semiconductors can only occurs if the CB of dye molecule is more negative than conduction band of semiconductors. In this mechanism when light falls on dye and

electrons jump to conduction band of semiconductors thus reducing the electron acceptor adsorbed on surface.

Kamet, et al. in 1989 reported the degradation of N,N,N,N-tetraethyloxamine by sensitized titania system.Anthrcine -9 carboxylic acid was used as a sensitizer which enhances response of titania into visible region. To regenerate the dye sensitizer redox couple was used. Such system can be used for oxidative degradation of dye sensitizers itself in absence of redox couple [6].

2.3.4 Transition Metal Doping:

Introduction of transition metal into semiconductor like titania is called transition metal doping and such metal is known as dopant.Semoiconductor doping with transition metal enhance the electron trapping. Doping of semiconductor with transition metal decreases the electron hole recombination rate by trapping the electron during illumination phase.Fe^{+3} and Cu^{+2} [7-8] inhibits electron hole recombination but not all transition metals decreases the electron hole recombination like Cr^{+3},because these transition metal produce acceptor and donor levels that causes direct recombination[9]

2.4 Zinc Telluride as a Photocatalyst:

Zinc telluride, semiconductor belonging II-VI group with narrow band gap of 2.26eV, has been widely studied in photocatalysis owing to its ability in solving environmental problems like air and water pollution [10]. But zinc telluride shows poor phtoctalytic activity particularly in visible light because of fast e^-/h^+ recombination. Apparently the efficacy of a semiconductor photocatalyst is dependent on the electron/hole recombination rate. In order to decrease the charge carrier recombination rate modification to semiconductor planes through addition of dopant, metal or combination with other semi-conductor are favorable and thus increases the photocatalytic behavior of photocatalyst. Various efforts were used to decrease the electron/hole recombination rate while promoting electron transfer in semiconductor which are discussed in section 2.3 [11].

Jun Zhang and Xiao-Ping (2015), were synthesized wurtzite phase zinc telluride with controllable aspects ratio using polytelluride as a precursor for tellurium. He also studied the effect of temperature on the morphology of zinc telluride while using polytellurides that allow the formation of wurtzite phase of ZnTe at relatively low temperature. The

kinetics and aspect ratio of nanocrystals growth of zinc telluride was controlled by tuning the temperature.UV-Vis spectroscopy was used to find the quantum confinement effect in ZnTe. Transient absorption measurements exhibit ultra-fast charge injection dynamics from zinc telluride nanorods, signifying their importance for phtocatalysis [12].

Jun zhang,Po- chiang chen and Ghouzhen shen (2008), were reported the synthesize of nanobelt zinc telluride that have electronic transport properties by passing the stream of argon at 250 ^{0}C in a three neck bottle fitted with condenser containing high boiling point liquid, oleylamine. The belt like morphology of zinc telluride was definite through field emission scanning electron microscopy and from XRD pattern. The FE-SEM image presented in given fig 1 clearly shows the belt like shape with the thickness less than 6nm and width 12nm approximately. The XRD pattern of nanobelt zinc telluride given in **fig 2.1 (b)** suggested single phase zinc blend structure [13].
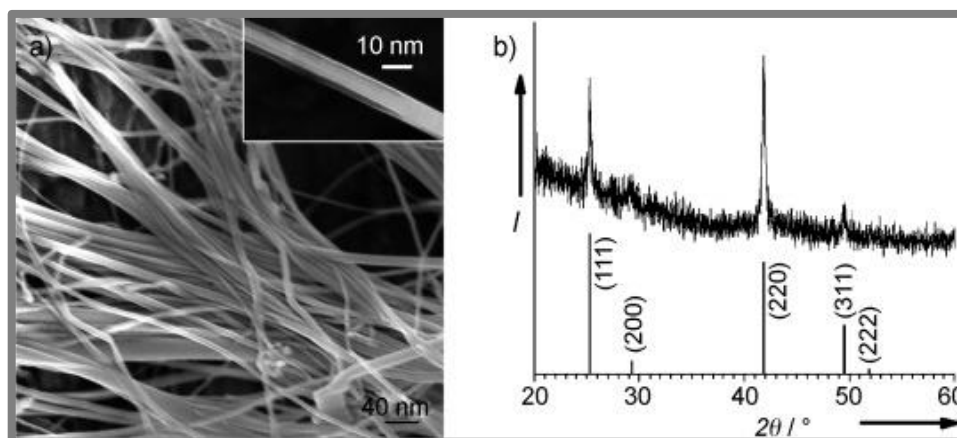
Fig 2.1 (a) SEM image of ZnTe nanobelt (b) XRD patterns of ZnTe nanobelts [13]

Yadong Li, Yi Ding, and Zhaou wang, synthesized zinc telluride via solvothemal method using zinc and tellurium powder as the reactants and hydrazine hydrate as the solvent which provide electron transfer medium. Analysis of results exhibited that the yield of this method is up to 90% and the produce zinc telluride showed nanorod morphology [14].

Linrui Hou, et al. used interfacial synthetic strategy, by reacting zinc acrylate with NaHTe at 90^{0}C upon the toluene-water interface, for synthesizing ZnTe single crystalline

nanorods .During this synthesis long alkyl chain fatty acids was used as a capping ligand. The as-synthesized zinc telluride nanorods showed stable blue fluorence up to 60% quantum yield, allowing them to be widely us in various applications like LED [15].

Yutang Liu, et al. described the synthesis of ZnTe/TiO$_2$ based composites through pulse deposition of zinc telluride on to upper surface of titania nanotubes array and also checked their photocatalytic degradation activity towards anthracene 9-carboxylic acid. It was confirmed from the results that nanoparticles of zinc telluride are evenly distributed over the upper surface of titania nanotubes. The zinc telluride modified titania nanotubes shows high photo catalytic activity as compared to unmodified titania nanotubes towards anthracene 9-carboxylic acid. The increased photocatalytic activity was found from the improved photocurrent density and from the presence of zinc telluride which reduces the hole/electron recombination rate [16].
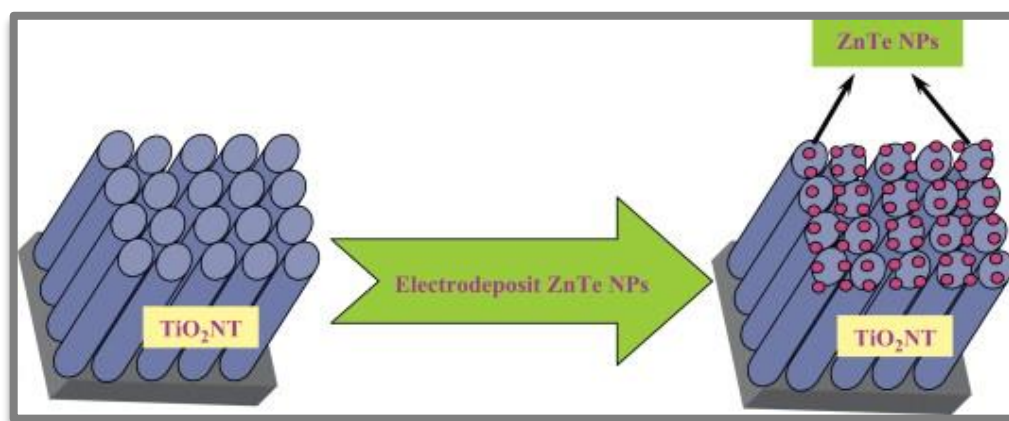
Scheme 3: Electro deposition of ZnTe nanoparticles on TiO2 nanotubes [16]

Xiao-Ping wu, JieGu and Shao-Min Zhou (2014), followed solvothermal method, using different sources of zinc, ethylene glycol as a solvent and sodium hydroxide for synthesizing redbay berry like microstructure of zinc telluride. The effect of reaction reagent like sodium hydroxide on the morphology of zinc telluride was also discussed. When the amount of sodium hydroxide increased from .2g to .8g the attained sample changed from nanowires to redbay berry like structure. They suggested that hydroxyl ion

controlled the morphology of obtained microstructure. Red bay berry microstructure of zinc telluride showed high photocatalytic activity towards methyl orange up to 90% as compared to microsphere ZnTe which is because of high surface area of red bay berry ZnTe microstructure, allowing them to played important role in environment purification [17].

Xiaxiaoping Wu, et al. testified the synthesis of microsphere zinc telluride with a mean diameter of 600nm via solvothermal method. Individual microsphere is composed of primary nanoparticles having diameter 30nm.Photo-assisted conductive atomic force microscopy was used to calculate the photoelectric effect of single zinc telluride microsphere, which showed the bigger current under UV light which is 28.7 times higher than that under dark field .The as-prepared microsphere zinc telluride showed excellent photo response conducting property which will make such materials countless in different application like photocatalysis and solar cells [18].

Muhammad Fahad Ehsan and Tao He (2014), were synthesized common cation ZnO/ZnTe heterostructure via hydrothermal method through modification of ZnO by ZnTe at 180 ^{0}C.The as syntheized ZnO/ZnTe heterostructure exhibits good photo reduction, even 3.28% solar conversion efficiency was observed for sample containing approximately 3.35% zinc telluride in terms of atomic percentage. High photocatalytic activity was attributed to the formation of hetrojunction which facilitate the charge transfer under visible light [19].

2.5 N-Doped Reduced Graphene Oxide Based Nanocomposites:

Dr Zhigang Xing, Li Li Zhang and Prof Xio Song (2011), prepared the copper modified reduced graphene oxides via immersion method. The presence of copper crystalline species over RGO surface was confirmed through the XRD, SEM, TEM and photoelectron spectroscopy. Bare reduced graphene oxide degraded the Rhodamine B under visible light but with slow rate. The photocatalytic activity of copper modified graphene towards Rh-B under visible light was higher than that of gold modified graphene. The high photocatlytic activity was because of copper, transferring the excited electron from reduced graphene oxide sheets to adsorbed oxygen producing reactive oxygen species for the waste water purification [20].

Hui Zhang, et al. were reported the synthesis of graphene sheet grafted Ag-AgCl hybrid plasmonic photocatalyst through precipitation method using silver nitrate as a precursor for silver. Four folds enhancement in photocatalytic activity was detected under visible light irradiation for Ag-AgCl/RGO photocatalyst towards RhB as compared to bare Ag-AgCl. The increase in activity was attributed to actual charge transfer from silver nanoparticles to reduce graphene oxide sheet which reduces the recombination rate of charge carrier through photocatlytic process [21].

Mingiun Zhou, Donglai Han and Xinlin Liu, used hydrothermal method, where the production of earth metal doped cadmium selenide nanoparticle and reduction of graphene oxide sheet occur at the same time, for synthesis of alkaline earth metals doped cadmium selenide reduced graphene oxide hybrid structure. The as-synthesized quantum dots cadmium selenide/RGO showed good photocatalytic activity and stability towards tetracycline chloride solution up to 85.6%, the morphology and structure confirmed, the high photocatalytic activity of as synthesized Ca^{+2} doped CdSe/RGO [22].

Shixiong Min and Gong Xuan Lu, presented a dye-sensitized photocatalysis scheme for hydrogen evolution from water reduction by using platinum modified reduce graphene oxide nanoparticles. The electron accepting and transferring behaviors of reduce graphene oxide simplify the e^- transfer from excited dye to catalyst platinum, retard the recombination of charge carriers due to which photocatalytic rate increases for hydrogen evolution [23].

Zhiyong Gao (2011), reported graphene cadmium sulphide nanocomposites via solvothermal method using ethylene glycol as a solvent at $100\,^0C$ for 24hr. Ethylene glycol help in the formation of cadmium sulphide nanoparticles and also causes the reduction of GO. Morphology of G-CdS nanocompoites was confirmed through SEM which shows that nanosphere CdS grow uniformly on the sheet of graphene, with the size 90nm. The high photodegradation towards RhB and stability of as synthesized G-CdS composites confirmed the good photo catalyst in visible light.[24].

Kun Chang, Zongwei and Tao Wang, were synthesized MoS_2/graphene co-catalyst for photocatalytic water splitting. The as-Prepared composite MoS_2/G-CdS was annealed at 573K in argon atmosphere for 2hrs. From different characterization methods it was

confirmed that cadmium sulphide nanoparticles were equally distributed on the surface of MoS$_2$/G hybrid. High photocatalytic hydrogen production activity under visible light irradiation was observed when the molar ratio of MoS$_2$ to graphene was 1:2 and MoS$_2$/graphene catalyst was 2.0wt% [25].

Hui Liu, et al. (2014), were used a two-step hydrothermal process for preparation of core shell structure CdS/RGO at 180 ^{0}C for one hour. The obtained sample was analyzed through XRD, SEM and IR all these technique confirmed that the core shell structure composites indicate a uniform morphology and size. The as-prepared sample exhibit high degradation rate up to 95.2% as compared to pure CdS towards dye RhB in just 50 mint. The high activity was because of stepwise energy level and high surface area of the obtained photocatalyst that increases the adsorption ability of dye molecule and suppressing the charge recombination of photocatalyst. It was also reported in literature that introduction of graphene shell shield the CdS microsphere from photo corrosion [26].

Weilin Wang,Zhaofeng Wang and Jingiing Li, were prepared TiO$_2$-S/RGO via one step hydrothermal method at 180 ^{0}C for 24 hrs using titanium n-butoxide as a precursor for titania.Doping in titania was done in order to reduce the band gap and make them visible light active and incorporation of RGO reduces the recombination of charge carriers. The high photodegradation activity towards methylene blue under simulated light was observed for TiO$_2$-S/RGO as compared to sulphur doped titania and bare titania [27].

Marilyn Yuen Sok Wen1, Abdul Halim Abdullah1, and Lim Hong Ngee, were reported synthesize of ZnO/RGO with varying GO content through precipitation method. The obtained dried powder of ZnO/RGO was calcinated at 400 °C for two hours. The band gap energy and surface area of ZnO/RGO nanohybrid was found smaller than that of pure zinc oxide. All the nanohybrid of ZnO/RGO showed high photodegradation activity towards methyl orange than bare ZnO. ZnO/RGO10 (with volume ratio of 10:100) showed four times higher activity than bare ZnO which was because of effective charge transfer to graphene sheet that reduces charge recombination rate [28].

Koushik Chakraborty, et al. (2018), were used solvothermal method for synthesis of RGO-ZnTe composites. Mixture of ethylenediamine and ethylene glycol was used as a solvent during their synthesis. Photoluminescence analysis of as prepared photocatalyst confirmed the efficient transportation of photo induced electron from zinc telluride to reduced graphene oxide sheet that reduces the charge recombination rate. The obtained sample RGO/ZnTe showed 6 times higher photocatalytic activity compared to bare RGO and 2.6 times compared to pure zinc telluride towards tetracycline antibiotics degradation under visible light. The high degradation activity towards tetracycline antibiotic was due to better interaction and synergic effect between reduced graphene oxide and zinc telluride. It was also reported in literature that oxygen and holes are the responsible reactive species for TC degradation [29].
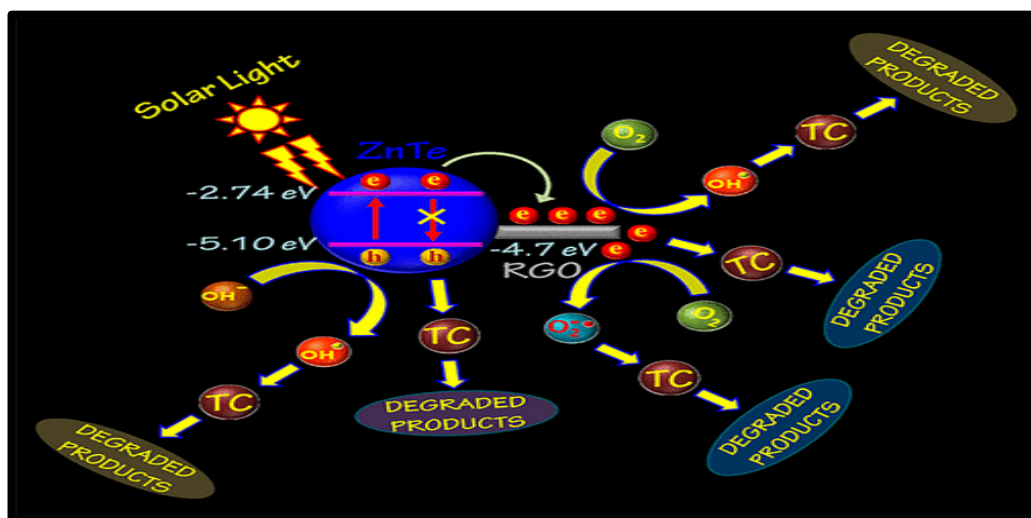
Scheme 4: Schematic illustration of antibiotic degradation by RGO-ZnTe [29]

Kouroshi Rahimi, Haniyeh Zafarkish and Ahmad Yazdani, were synthesized RGO-NiO nanowires via thermal decomposition followed by reduction of Ni (II) oxalate dihydrate in the presence of GO nanosheets.The obtained catalyst was analyzed for their photodegradation activity on MO. It was reported that introduction of reduce graphene oxide sheet reduces the band gap energy of nickel oxide and reduces the electron hole recombination rate in RGO-NiO composites as compared to bare NiO nanowires, making them good photocatalyst compared to that of standard TiO_2-P25 [30].

Brindha Appavu, Siva Kumar and Sudhakar, reported the synthesis of novel N-doped RGO/BiVO$_4$ using hydrothermal method at 180^0C for 24hrs.Urea was used as precursor for nitrogen doping in reduced graphene oxide. The XRD, TEM, SEM, UV-Vis, IR, XPS nitrogen adsorption and desorption and EIS techniques were used to check the physiochemical properties of as-synthesized sample. The obtained photocatalyst were used for both degradation of organic dyes and antibiotic. Both the antibiotics (metronidazole and chloramphenicol) and dyes (Congo red and methylene blue) was maximum degraded through N-RGO/ BiVO$_4$.The high photodegradation rate was observed for N-RGO/BiVO$_4$ then RGO/BiVO$_4$ and bare BiVO$_4$ .In N-RGO/BiVO$_4$ graphene oxide facilitated the transportation of electrons and charge separation. Due the presence of N-RGO the photo generated species generate the superoxy and hydroxyl radicals afore recombination as a results composite photocatalyst shows higher photo catalytic activity as compared to their pure counterparts [31].

M.Mohamed Jaffer Sadiq,et al. (2018), reported the synthesis of ternary nanocomposites of NiWO$_4$-ZnO-NRGO via microwave irradiation method. Different methods were used to study the surface morphology, optical properties, phase purity and elemental composition of prepared catalyst. The catalyst were used for both degradation of methyl blue dye and also for reduction of 4-nitrophenol to 4-Amino phenol in presence of NaBH$_4$. The photocatalytic activity of nanocomposites under visible light was 9 times more than bare NiWO$_4$, their entire studied showed that as synthesized ternary nanocomposites can be used for bioremediation and industrial purposes [32].

Hai-Xia, Rong Wu and Hang We (2016), reported the photodegradation activity of zinc telluride- reduce graphene oxide composites under visible light. Solvothermal method was used for their synthesis.N$_2$H$_4$ used as a reducing agent, not only stimulated the formation of zinc telluride but also reduced the graphene oxide to reduced graphene oxide. Methylene blue was degraded through obtained catalyst under visible light. RGO/ZnTe proved to give the best results as compared to bare ZnTe. These studied also reported the mechanism of enhance photodegradation activity of ZnTe/RGO as the conduction band of ZnTe/RGO is more negative than conduction band of reduced graphene oxide as a result the electron can transferred to the RGO sheets, thus reducing the electron/hole

recombination rate in zinc telluride while the accumulated electrons on the RGO surface convert dissolve oxygen into oxidative species which degrade the organic pollutant [33].

Figure 2.2: Formation of ZnTe/RGO [33]

Qian Mi., Daiquan Chen and Uncheng Hu (2013), were synthesized N-doped graphene/CdS hollow spheres nanocomposites via one pot template free method. N-graphene had sheet like morphology with interlayer distance about .34nm confirmed through scanning electron microscopy. The as synthesized composites has shown good stability and activity towards MB dye up to 94% as compared to GO/CdS and bare CdS.The increased photocatalytic activity was found due to N-graphene that acts as excellent electron transporter and acceptor [34].

References:

[1]. Fujishima, Akira, Xintong Zhang, and Donald A. Tryk. "TiO_2 photocatalysis and related surface phenomena." *Surface Science Reports* 63.12 (2008): 515-582.

[2]. Struve and Walter S. *Fundamentals of Molecular Spectroscopy*, (1989): 245-248.

[3]. Atkins, Peter W., and Ronald S. Friedman. *Molecular Quantum Mechanics*, (2011): 789-799

[4]. West, Paul R., Juntao Li, Rongbin Su and Beimeng Yao. "Searching for better plasmonic materials." *Laser and Photonics Reviews* 4.6 (2010): 795-808.

[5]. Gopidas, K. R., Maria Bohorquez, and Prashant V. Kamat. "Photophysical and photochemical aspects of coupled semiconductors, charge-transfer processes in colloidal cadmium sulfide-titania and cadmium sulfide-silver (I) iodide systems." *Journal of Physical Chemistry* 94.16 (1990): 6435-6440.

[6]. Spanhel, Lubomir, Horst Weller, and Arnim Henglein. "Photochemistry of semiconductor colloids, electron ejection from illuminated cadmium sulfide into attached titanium and zinc oxide particles." *Journal of the American Chemical Society* 109.22 (1987): 6632-6635.

[7]. Li, and Xiaobo. "Photophysical and photochemical investigations of new tunable luminescent metl-metal bonded exciplexes."*Material and Design* (2011): 184-194

[8]. Fujihira, Masamichi, Yoshiharu Satoh, and Tetsuo Osa. "Heterogeneous photocatalytic reactions on semiconductor materials. Effect of pH and Cu^{2+} ions on the photo-Fenton type reaction." *Bulletin of the Chemical Society of Japan* 55.3 (1982): 666-671.

[9]. Herrmann, Jean-Marie, Jean Disdier, and Pierre Pichat. "Effect of chromium doping on the electrical and catalytic properties of powder titania under UV and visible illumination." *Chemical Physics Letters* 108.6 (1984): 618-622.

[10]. Wu, Xiao-Ping, Jie Gu, Shao-Min Zhou, and Xiao-Yun. "Red bayberry-like ZnTe microstructures: controlled synthesis, growth mechanism and enhanced photocatalytic performance." *Journal of Alloys and Compounds* 627 (2015): 166-173.

[11]. Linsebigler, Amy L., Guangquan Lu, and John T. Yates Jr. "Photocatalysis on TiO$_2$ surfaces: principles, mechanisms, and selected results." *Chemical Reviews* 95.3 (1995): 735-758.

[12]. Hou, Linrui, Qiang Zhang, and Luting Ling. "Interfacial fabrication of single-crystalline ZnTe nanorods with high blue fluorescence." *Journal of the American Chemical Society* 135.29 (2013): 10618-10621.

[13]. Zhang, Jun, Po-Chiang Chen and Guozhen Shen. "P-Type Field-Effect Transistors of Single-Crystal Zinc Telluride Nanobelts." *Angewandte Chemie International Edition* 47.49 (2008): 9469-9471.

[14]. Li, Yadong, Yi Ding, and Zhaoyu Wang. "A novel chemical route to ZnTe semiconductor nanorods." *Advanced Materials* 11.10 (1999): 847-850.

[15]. Hou, Linrui, Qiang Zhang and Luting Ling. "Interfacial fabrication of single-crystalline ZnTe nanorods with high blue fluorescence." *Journal of the American Chemical Society* 135.29 (2013): 10618-10621.

[16]. Liu, Yutang, Xilin Zhang, Ronghua Liu, and Renbin. "Fabrication and photocatalytic activity of high-efficiency visible-light-responsive photocatalyst ZnTe/TiO$_2$ nanotube arrays." *Journal of Solid State Chemistry* 184.3 (2011): 684-689.

[17]. Wu, Xiao-Ping, Jie Gu, Shao-Min Zhou, and Xiao-Yun. "Red bayberry-like ZnTe microstructures: controlled synthesis, growth mechanism and enhanced photocatalytic performance." *Journal of Alloys and Compounds* 627 (2015): 166-173.

[18]. Wu, Xiaoping, Shaomin Zhou, Shiyun Lou and Yangquan Wang. "Solvothermal synthesis of ZnTe microspheres with enhanced light current." *Materials Letters* 83 (2012): 4-7.

[19]. Ehsan, Muhammad Fahad, and Tao He. "In situ synthesis of ZnO/ZnTe common cation heterostructure and its visible-light photocatalytic reduction of CO_2 into CH_4." *Applied Catalysis Environmental* 166 (2015): 345-352.

[20]. Xiong, Zhigang, Li Zhang, and Xiu Song Zhao. "Visible-light induced dye degradation over Copper-modified reduced graphene oxide." *Chemistry–A European Journal* 17.8 (2011): 2428-2434.

[21]. Zhang, Hui, Xinfei Fan and Xie Quan. "Graphene sheets grafted Ag-AgCl hybrid with enhanced plasmonic photocatalytic activity under visible light." *Environmental Science and Technology* 45.13 (2011): 5731-5736.

[22] Zhou, Mingjun, and Dongle Han, Xinlin. "Enhanced visible light photocatalytic activity of alkaline earth metal ions-doped CdSe/rGO photocatalysts synthesized by hydrothermal method." *Applied Catalysis B: Environmental* 172 (2015): 174-184.

[23]. Min, Shixiong, and Gongxuan Lu. "Dye-sensitized reduced graphene oxide photocatalysts for highly efficient visible-light-driven water reduction." *The Journal of Physical Chemistry* 5.28 (2011): 13938-13945.

[24]. Gaoli, Zhiyong, Ning Liu, Dapeng Wu and Wenguang Tao. "Graphene–CdS composite, synthesis and enhanced photocatalytic activity." *Applied Surface Science* 258.7 (2012): 2473-2478.

[25]. Chang, Kun, Zongwei Mei, Tao Wang, and Qing Kange. "MoS_2/graphene cocatalyst for efficient photocatalytic H_2 evolution under visible light irradiation." *ACS Nano* 8.7 (2014): 7078-7087.

[26]. Liu, Hui, Ting Lv, Xiao Hua Wu and Chunkui Zhu. "Preparation and enhanced photocatalytic activity of CdS-RGO core–shell structural microspheres." *Applied Surface Science* 305 (2014): 242-246.

[27]. Wang, Weilin, Zhaofeng Wang, Jingjing Liu, Zhu Luo. "Single-step one-pot synthesis of TiO_2 nanosheets doped with sulfur on reduced graphene oxide with enhanced photocatalytic activity." *Scientific Reports* 7 (2017): 46610.

47

[28]. Wen, Marilyn Yuen Sok, Abdul Halim and Lim Hong Ngee. "Synthesis of ZnO/rGO nanohybrid for improved photocatalytic activity." *Malaysian Journal of Analytical Sciences* 21.4 (2017): 889-900.

[29]. Chakraborty, Koushik, Tanusri P, and Surajit Ghosh. "Reduced graphene oxide supported zinc telluride, a graphene based composite for tetracycline degradation and their synergistic effect." *ACS Applied Nano Materials* 405 (2018): 252-259

[30]. Rahimi, Kourosh, Haniyeh Zafarkish, and Ahmad Yazdani. "Reduced graphene oxide can activate the sunlight-induced photocatalytic effect of NiO nanowires." *Materials and Design* 144 (2018): 214-221.

[31]. Appavu, Brindha, Sivakumar Thiripuranthagan, Sudhakar Ranganathan and Elangovan Erusappan. "BiVO$_4$/N-rGO nano composites as highly efficient visible active photocatalyst for the degradation of dyes and antibiotics in eco system." *Ecotoxicology and Environmental Safety* 151 (2018): 118-126.

[32]. Sadiq, M. Mohamed Jaffer, U. Sandhya Shenoy, and D. Krishna Bhat. "NiWO$_4$-ZnO-NRGO ternary nanocomposite as an efficient photocatalyst for degradation of methylene blue and reduction of 4-nitro phenol." *Journal of Physics and Chemistry of Solids* 109 (2017): 124-133.

[33]. Wang, Hai-Xia, Rong Wu and Shun-Hang Wei, Li-Rui Yu. "One-pot solvothermal synthesis of ZnTe/RGO nanocomposites and enhanced visible-light photocatalysis." *Chinese Chemical Letters* 27.9 (2016): 1572-1576.

[34]. Mi, Qian, Daiquan Chen, Juncheng Hu and Zhengxi Huang. "Nitrogen-doped graphene/CdS hollow spheres nanocomposite with enhanced photocatalytic performance." *Chinese Journal of Catalysis* 34.11 (2013): 2138-2145

Chapter 3

Experimental

Abstract:

This chapter explains all the practical work which was carried out for the synthesis of Zinc telluride, graphene oxide, Nitrogen doped reduced graphene oxide, and nano composites of N- doped reduced graphene oxide and zinc telluride. This chapter also explains the details of various techniques used for the characterization of as synthesized materials.

3.1. Synthesis of Zinc Telluride:

Hydrothermal method was used for synthesis of zinc telluride. The list of required chemicals is given below;

Table 3. 1: List of chemicals required for ZnTe synthesis

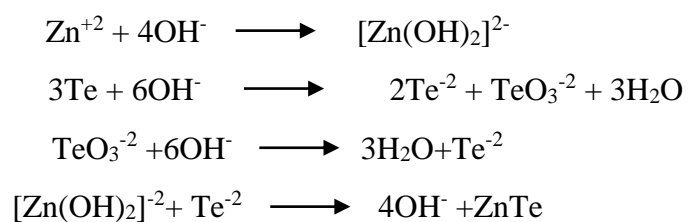| Chemicals	Purity	Company
Zinc powder	97%	Sigma-Aldrich
Tellurium Powder	99.8	Aldrich
Potassium hydroxide	85-100.5	Sigma -Aldrich

Procedure:

For the synthesis of zinc telluride, in the first step, 6.72g of potassium hydroxide were dissolved in 40ml distilled water and stirrer it.Then 1.3 g zinc powder and 1.53 g of tellurium powder were dissolved in a mixture obtained in first step and stir it with the help of glass rod until purple color appears. The mixture obtained then transfers to 40ml Teflon lined autoclaved and keep it in heating oven at 120 °C for two hours. After two hours, the autoclave was cooled down to room temperature. The black precipitates of zinc telluride were obtained which is washed with two times distilled water and one time with ethanol after its centrifuge in centrifugation machine at 11000rpm for 10 min per run. After washing the resulting blackish precipitate of zinc telluride were dried in vacuum oven at

120 °C for 24 hours. After drying and washing obtained zinc telluride nanoparticles were grinded and stored for further characterization and analysis.
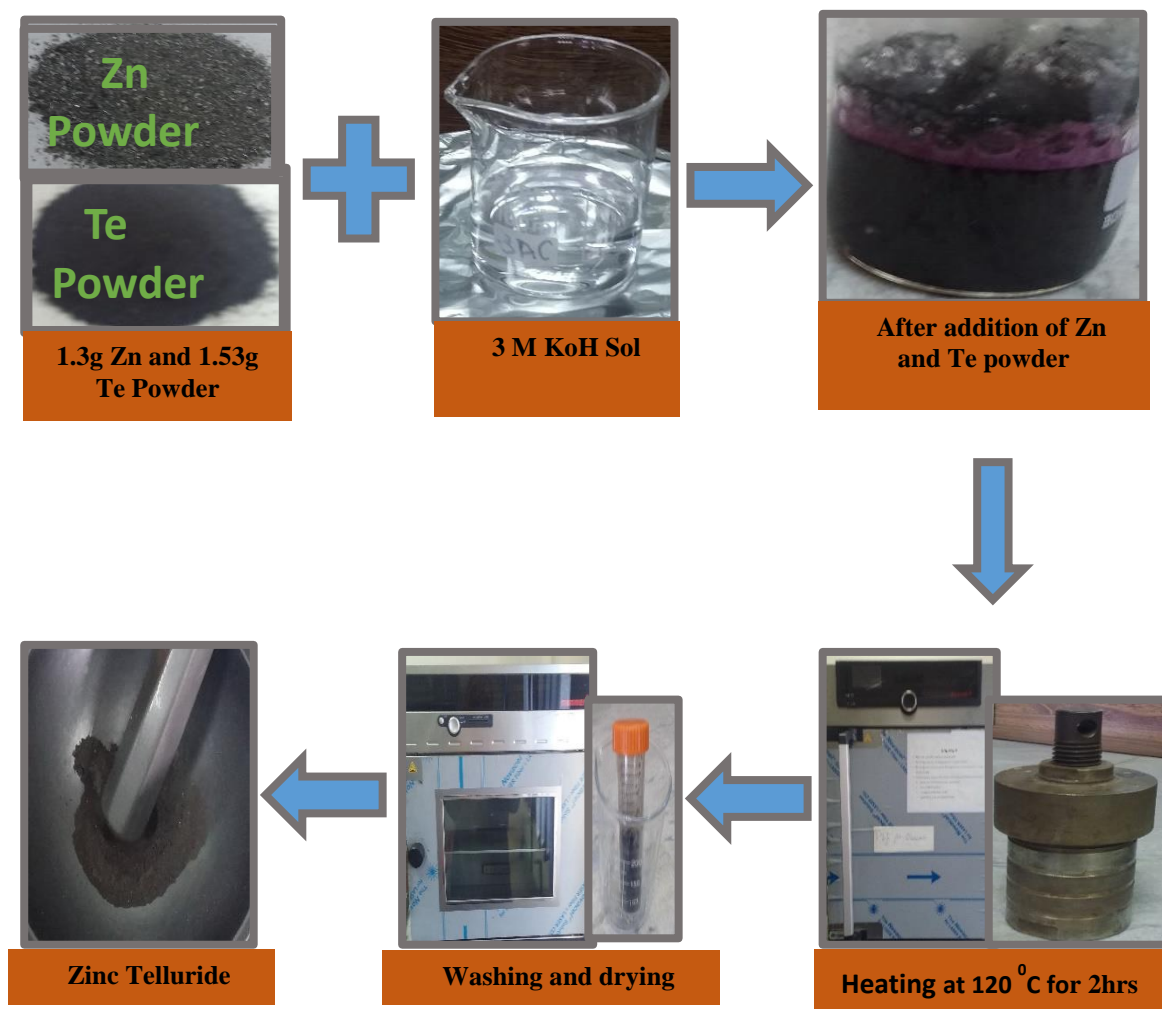
Scheme 5: Pictorial representation for ZnTe synthesis

The propsed synthesis scheme for zinc telluride is shown below;

$$Zn^{+2} + 4OH^- \longrightarrow [Zn(OH)_2]^{2-}$$

$$3Te + 6OH^- \longrightarrow 2Te^{-2} + TeO_3^{-2} + 3H_2O$$

$$TeO_3^{-2} + 6OH^- \longrightarrow 3H_2O + Te^{-2}$$

$$[Zn(OH)_2]^{-2} + Te^{-2} \longrightarrow 4OH^- + ZnTe$$

3.2. Synthesis of Graphene Oxide:

The chemicals used for synthesis of graphene oxide are listed in given table;

Table 3. 2: List of chemicals required for GO synthesis

| Chemicals	Purity	Company
Graphite Powder	99%	Sigma-Aldrich
Sodium nitrate	98%	Sigma-Aldrich
Potassium Permanganate	99%	Sigma -Aldrich
Sulphuric acid	98%	Sigma Aldrich
Hydrogen peroxide	40%,wt	Sigma Aldrich
Hydrochloric acid	35%	Sigma Aldrich

Procedure:

Hummers' Method was used for synthesis of graphene oxide which involved the oxidation of graphite flakes. For synthesis of graphene oxide, 2g of graphite powder and 2g of sodium nitrate were taken in 1000mL beaker, then 50mL of sulphuric acid was added in it and beaker was kept in an ice bath at 0- 5^0C with constant stirring. The mixture was stir for two hours at 0- 5^0 C. After two hours, 6g of potassium permanganate were added slowly that give greenish color to the reaction mixture. As the addition of $KMnO_4$ can rise the temperature of mixture so ice bath was not removed in order to maintain the temperature. The ice bath was then removed after addition of $KMnO_4$ under constant temperature (below 15^0C) and the resulting mixture was kept under stirring for two days. Chocolaty thick mixture was observed after two days stirring to dilute the reaction mixture 100mL of deionized water were added slowly, temperature should be maintained below 35 ^{0}C. For further dilution 200mL of water were added to the reaction mixture under continuous stirring. The addition of water changes the color of reaction mixture from gray to brown. To terminate the reaction mixture 10mL of hydrogen peroxide were added drop

wise that give yellow color to the reaction mixture. The resulting mixture was then centrifuged at 6000rpm and washed with 10%HCl and several times with deionized water for purification purpose. After washing the resulting product were dried in vacuum oven at 35 ^{0}C for 24 hours. The dark brow to blackish flakes were obtained after drying which was grinded and stored in air tight vials for further characterization and analysis. Given in scheme are the processes that were performed while preparation of graphene oxide nanosheets.
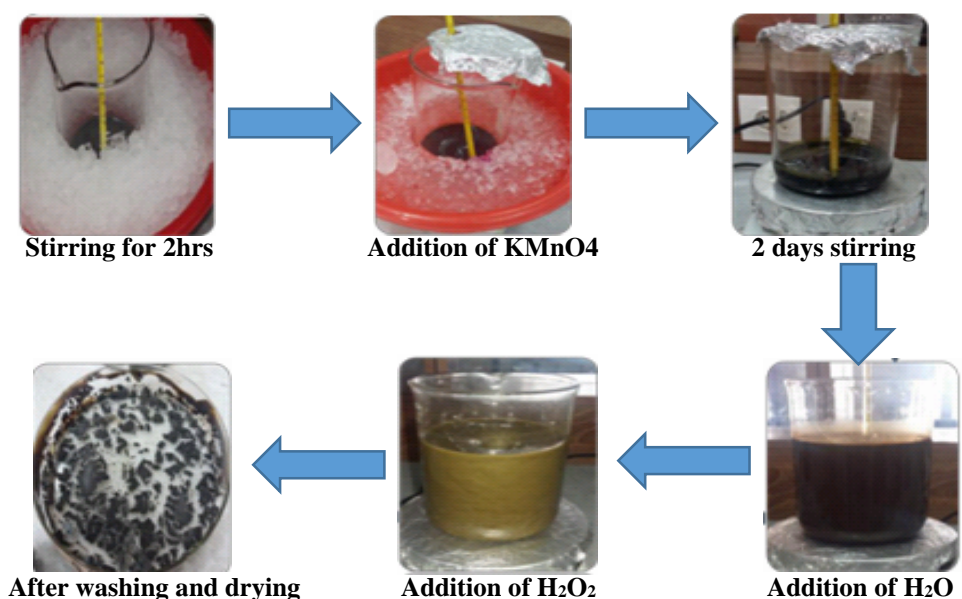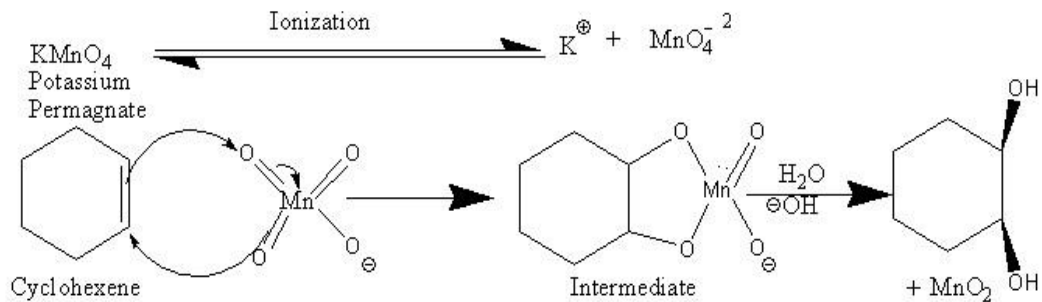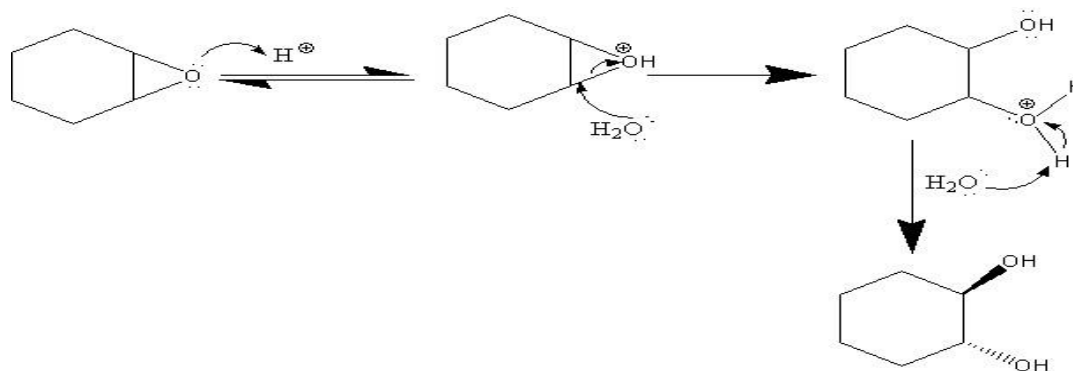

Scheme 6: Synthesis of graphene oxide

Formation of di-manganese heptaoxide from potassium permanganate in presence of strong acid is shown below [48];
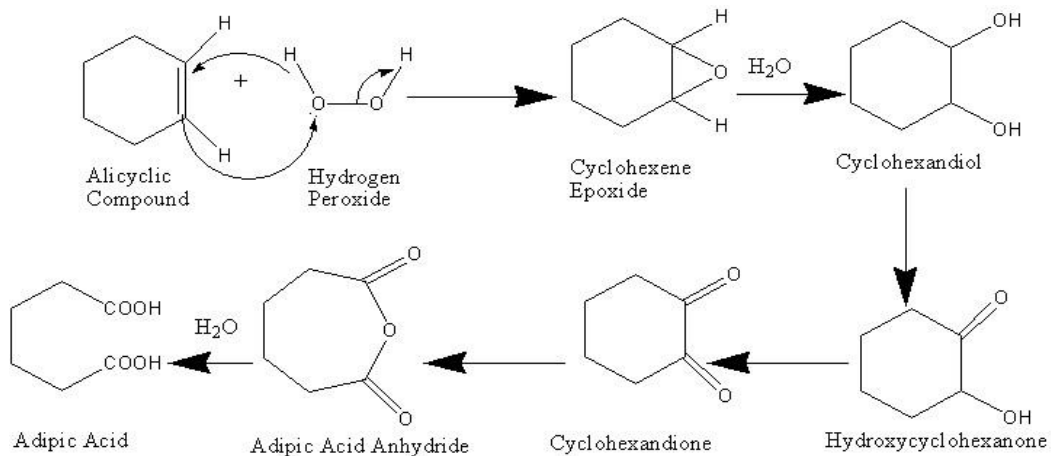
$$H_2SO_4 + KMnO_4 \rightarrow K^+ + MnO_3^+ + H_3O^+ + HSO_4^-$$

$$MnO_3^+ + MnO_4^- \rightarrow Mn_2O_7$$
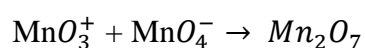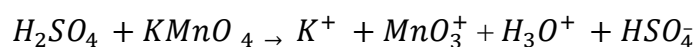
3.2.1 Oxidation Mechanism:

Mechanism of cis-diol formation by potassium permanganate

Mechanism of trans-diol formation by hydrogen peroxide

Mechanism of oxidation by H_2O_2

3.3. Synthesis of N- Doped Reduced Graphene Oxide (N-RGO):
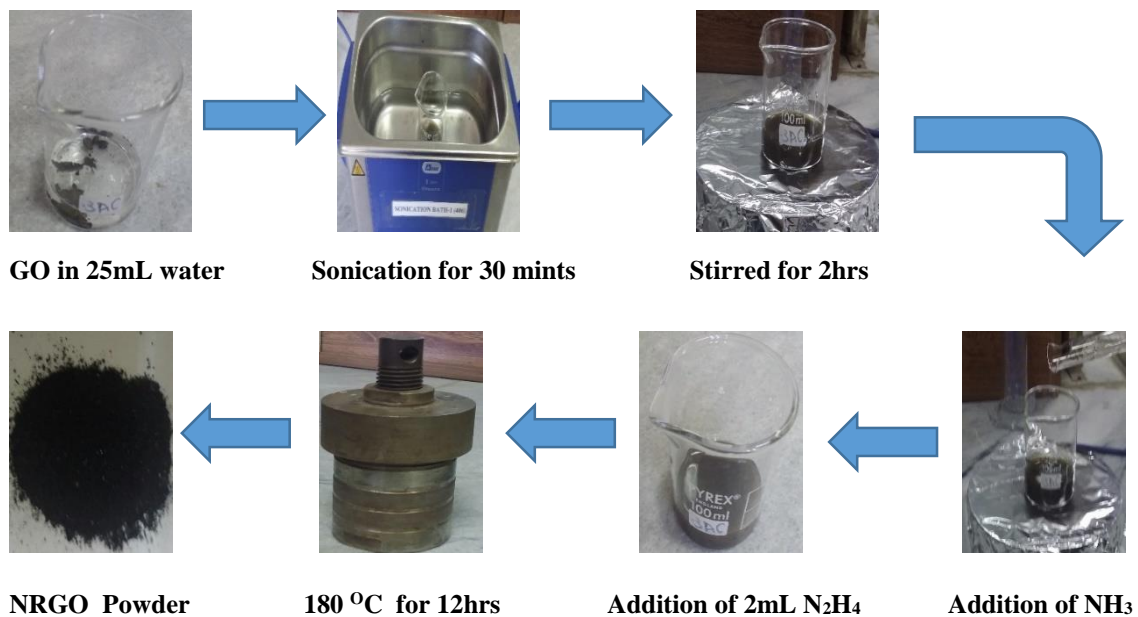
The chemicals used for synthesis of Nitrogen doped reduced graphene oxide is listed in given table:

53

Table 3. 3: List of chemicals required for NRGO synthesis

Chemicals	Purity	Company
Hydrazine hydrate	99%	Merck
Graphene oxide	From purified graphite	Hummers Method
Deionized water	99%	Sigma Aldrich
Ammonia solution	98.9%	Aldrich

Procedure:

For synthesis of N-RGO hydrothermal method was used in which the nanomaterials are prepared at elevated pressure.In the first step,2g of graphene oxide as prepared through Hummers method in 100mL beaker were taken 25mL of deionized water was added in it and to make the homogenous dispersion the solution is sonicated in sonication bath for 30 minutes.The resulting solution was then placed at hot pate and kept on stirring for 1 hour. After 1 hour stirring 13mL of ammonia solution (prepared by dissolving 2mL of ammonium hydroxide in 12mL of deionzed water) was added into the reaction mixture and stirred for 15 minutes, then 2mL of hydrazine hydrate was added into the above mixture.The above mixture was then shifted into teflon cup and kept it in heating oven at 180 ^{0}C for 12 hours.Finally,the resullting precipitates of N-RGO was washed with deionized water and ethanol after its centrifuge in centrifugation machine at 11000rpm for 15 minutes. After washing the mixture is dried in vacuum oven at 60 ^{0}C for 24 hours.The sample was finally prepared after drying and grinding which was further used in the synthesis of nancomposites and photocatalytic activity.

GO in 25mL water	Sonication for 30 mints	Stirred for 2hrs
NRGO Powder	180 ^{O}C for 12hrs	Addition of 2mL N_2H_4	Addition of NH_3

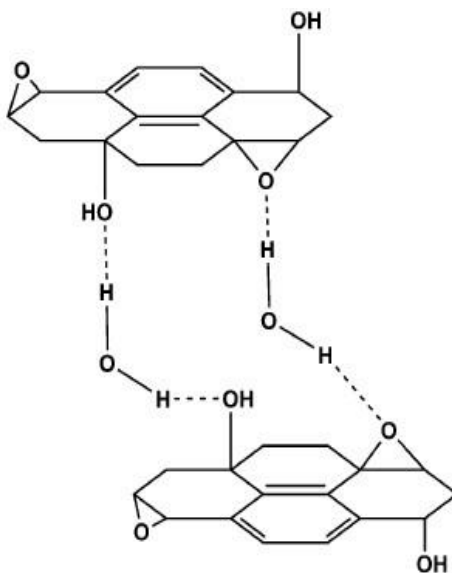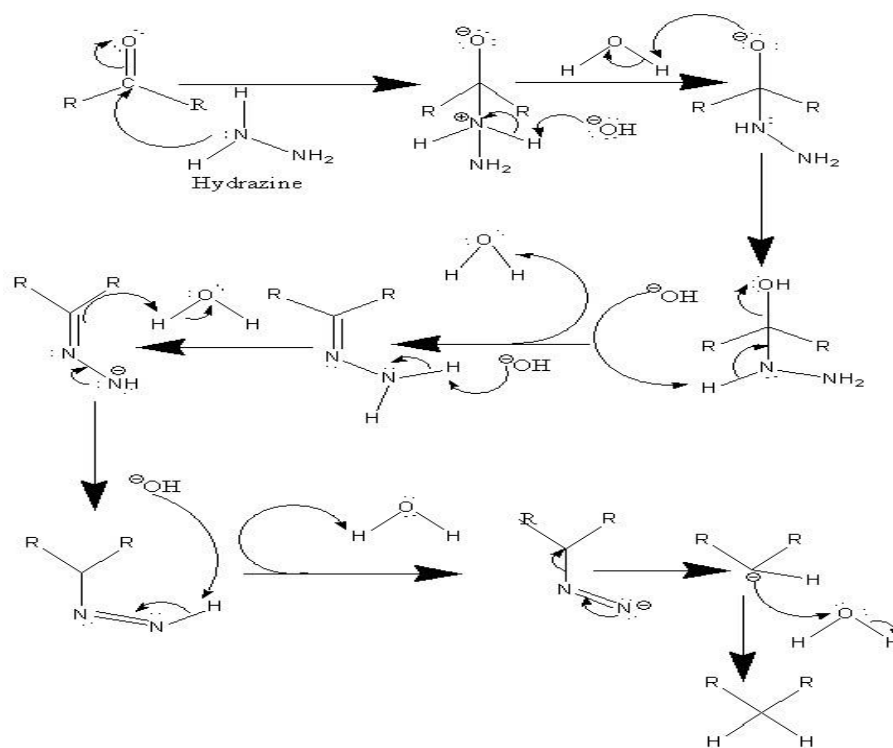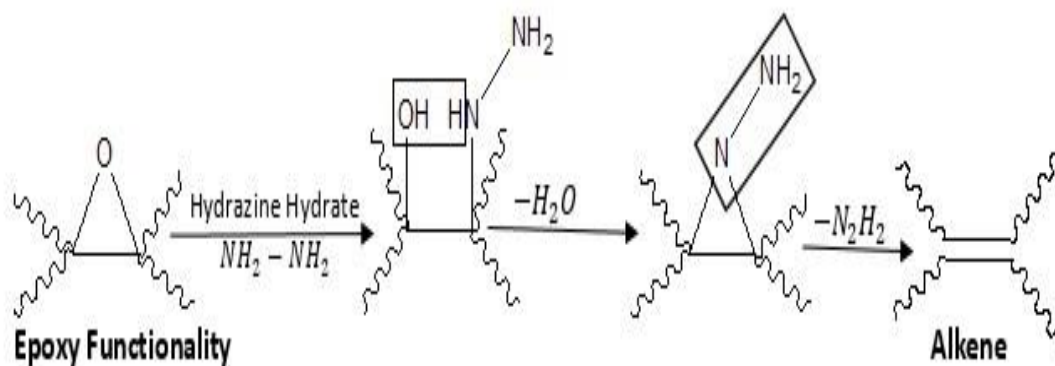**Scheme 7: Synthesis of N-doped reduced graphene oxide**

Fig 3.1: Hydrogen bonding between graphene oxide and water [49]

3.3.1 Reduction Mechanism:

Reduction mechanism for carbonyl functionality [49]

Reduction mechanism for epoxy functionality [49]

3.4 Synthesis of Zinc Telluride Nitrogen Doped Reduced Graphene Oxide Nanocomposites:

For synthesis of all nanocomposites having stiochiometeric ratio of 1:3 ,1:1, and 3:1 of ZnTe and N-RGO respectively physical method was employed. Physical method involves

the simple mixing of both prepared catalyst by grinding. For synthesis of 1:3 ZnTe-NRGO, 0.25g of as synthesized ZnTe and 0.75g of N-RGO powder was grinded for one hour using agate mortar and pestle. Same procedure was followed but with different ratio of zinc telluride and n-doped reduced graphene oxide.For synthesis of 1:1 ZnTe-NRGO (.25g ZnTe and .25g NRGO) and for 3:1 ZnTe-NRGO (.75g ZnTe and .25gNRGO) of as prepared catalyst was ground in agate mortar and pestle for one hour.Indices of samples and experimental detail is shown in given table

Table 3.4: Synthesis of nanocomposites with different stiochiometeric ratio

ZnTe by wt%	NRGO by wt%	Sample ID
0	100	NRGO
25	75	1:3 ZnTe-NRGO
50	50	1:1 ZnTe-NRGO
75	25	3:1 ZnTe-NRGO
100	0	ZnTe

3.5 Photocatalytic Measurement:

The photocatalytic activity of synthesized pure and composites photocatalyst was calculated in the photodegradation of CR dye in an aqueous solution in the illumination of visible light. Halogen lamp was used as a source visible light. The photocatalytic action of all the prepared samples towards Congo red dye was performed in batch type reactor. In a characteristic experiment, 0.01g of photocatalyst was dissolved in 100mL of CR dye solution of (50 mg / L in water). The solution was then kept under stirring for one hour in dark to attain an adsorption-desorption stability between dye and photocatalyst. During irradiation an amount of 3mL of test samples were taken at regular interval of time and were immediately centrifuged to isolate the particles of catalyst. The concentration of CR in test samples was determined at 497nm.

Chapter 4
Results and Discussions

Abstract:

This chapter discusses the results through various characterization techniques as already detailed in the abstract. In addition, the photocatalytic activity of the as-synthesized nanomaterials is also discussed here.

4.1 Phase Analysis:

The XRD pattern of as prepared ZnTe, GO, RGO, NRGO and ZnTe - N-RGO are displays in **fig 4.1.** In **fig a**, GO show a sharp diffraction peak at angle 10.5^o corresponding to (001) plane, revealed the successful oxidation of original graphite [1]. The XRD spectra of RGO shows one dominant band corresponds to (002) at 26.5^0 and one weak band appeared at 43.4^0 along (100) plane, shows the reflection of un-oxidized graphite present in case of both RGO and N-RGO [2].The characteristic peak of GO which appear at (001) plane is not observed in the diffraction pattern of RGO and NRGO confirming the complete reduction of graphene oxide, eliminating the oxygen containing function group and exfoliation. However in the XRD spectra of RGO and NRGO negligible difference was observed indicating that nitrogen doping probably had no effect on the layers of RGO due to its small concentration [3]. In given **fig (g)** shows the XRD spectra of ZnTe which is well matched with literature (JCPDS # 0650385), prepared at 120 ^{0}C for two hours through hydrothermal route. All the peaks appeared at 25^0, 29^0, 42^0, 50^0,61^0,67^0 Corresponds to (111), (200), (220), (311), (400), (420) plane of ZnTe, confirm cubic structure of ZnTe with lattice constant of 6.128 A^0 and lattice angle of 90°. Moreover, this fig shows the results of nano composites and prepared catalyst with different ratio (3:1, 1:1, and 1:3). The disappearance of characteristic diffraction peak at 10.4^0 in nanocomposites confirmed that GO has been reduced. However, the peak matching to N doped RGO is not detected in the XRD pattern of nanocomposites this can be, either the main peak of NRGO at 26.5^0 could be overlapped by the peak of ZnTe appeared at 25^0 or may be due to small amount of N doped RGO in nanocomposites [4].
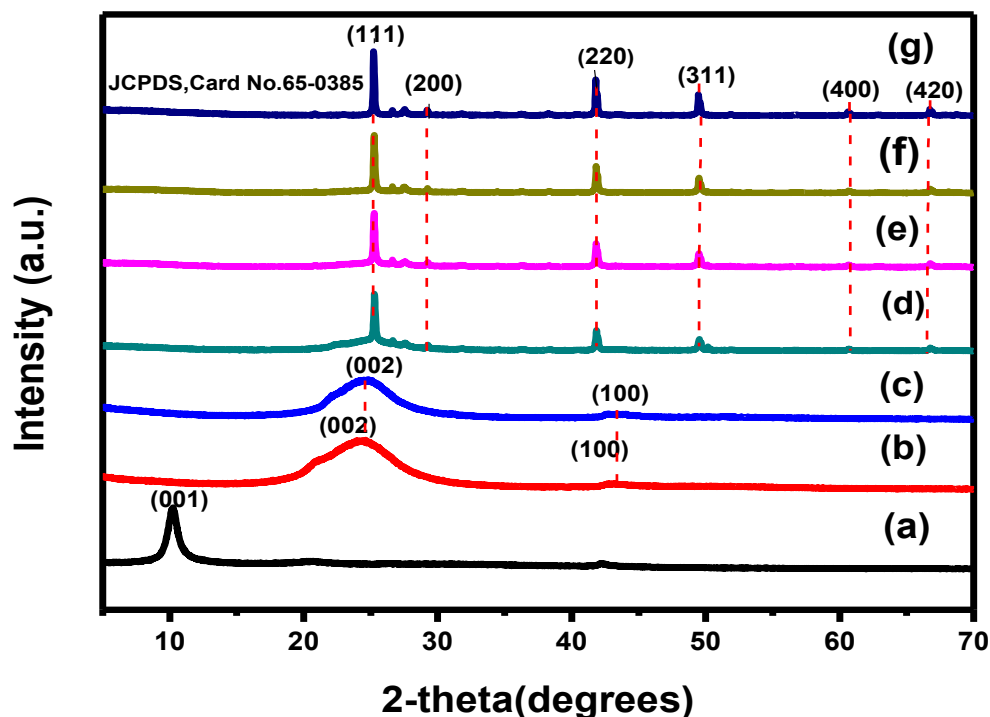
Fig.4.1: XRD Patterns of (a) GO (b) RGO (c) NRGO (d) 1:3 ZnTe-NRGO (e) 1:1 ZnTe-NRGO (f) 3:1 ZnTe-NRGO and (g) ZnTe

4.2 Morphological Analysis:

To confirm the particle size and morphology of as prepared catalyst SEM analysis was carried out, for this VEGA$_3$LaB$_6$ TESCAN machine were used present at USP-CASE, NUST which is also coupled with energy dispersive spectroscopy to allow the elemental compositional analysis of a sample. SEM image in **fig 4.2 (d)** shows that NRGO sheets are rippled and tangled with each other forming wrinkled sheet like structure having thickness in micrometer range but its thickness can be in nanometer range depending on the number of stacked sheets [5]. **Fig 4.2 (a), (b), and (c)** shows SEM micrographs of nanocompoistes, which exhibits that by making the composites the graphene sheet got stretched, due to presence of ZnTe.
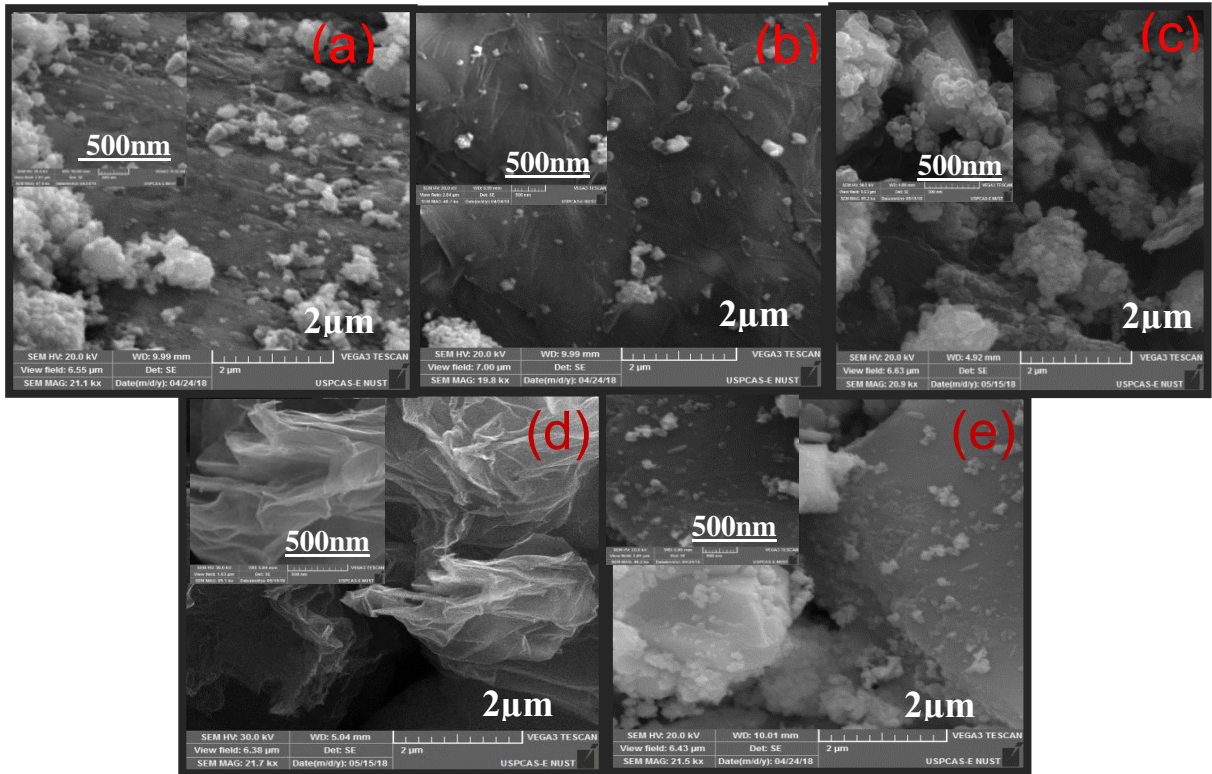
Fig.4.2: SEM images of (a) 1:3 ZnTe-NRGO (b) 1:1 ZnTe-NRGO (c) 3:1 ZnTe-NRGO and (d) N-doped RGO (e) ZnTe

We can see in **fig 4.2 (b)** the nanoparticles of zinc telluride are uniformly decorated on the surface of nitrogen doped RGO without any formation of agglomerates. A lot of electro negative groups are present in nitrogen doped RGO that provides the nucleation sites for the growth of nanoparticles as a results prevent the nanoparticles from aggregation [6]. As the concentration of NRGO decreases or increases during nanocomposites formation it causes the aggregation of nanoparticle on surface of graphene sheets which can be clearly seen in **fig 4.2 (a) and (c)**.The SEM image of ZnTe which was prepared via hydrothermal method at $120\,^0C$ for 2 hours suggest that particles have approximately irregular large and small spherical shapes where mostly unite to form large agglomerates as shown in **fig 4.2 (e).**

4.3 Compositional Analysis:

The EDX Spectra of all the prepared samples were analysis by TESCAN machine. Energy dispersion spectroscopy is used to measure the elemental composition of the sample. EDX analysis of all the prepared catalyst is shown in given figures. Only peak of Zn and Te are present in the EDX spectrum of pure ZnTe which can be seen in **fig 4.3,** confirming the purity of synthesized sample. Moving towards the results of nanocomposites, EDX analysis in **fig 4.5.4.6 and 4.8** shows the presence of C, O, Zn, and Te element in each prepare catalysts. The prepared sample contained zinc telluride and N-doped RGO with different stoichiometric ratio that is 1:3, 1:1, and 3:1 respectively. From percentage composition of all the nanocomposites, given in table 4.1, it can be seen as the ratio of NRGO decreases then the ratio of carbon to oxygen also decreases. **Fig 4.4** shows the EDX spectrum of NRGO, all the peaks in the spectrum corresponds to C and O with atomic % 92.15 and 7.85 respectively, confirming the impurity free synthesis of NRGO. However there is no peak observed for nitrogen in all the prepared samples as the weight of nitrogen is very low and its amount cannot be observed.
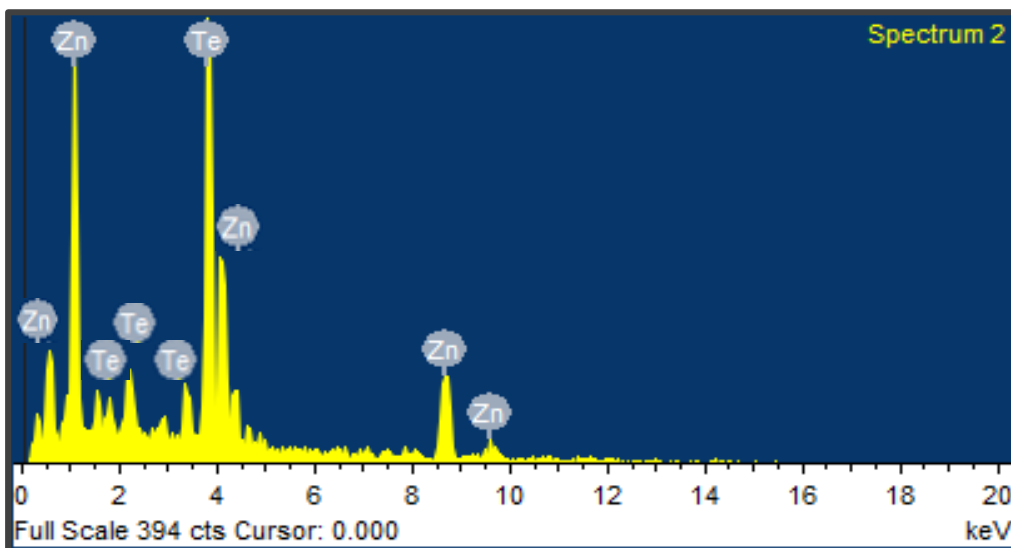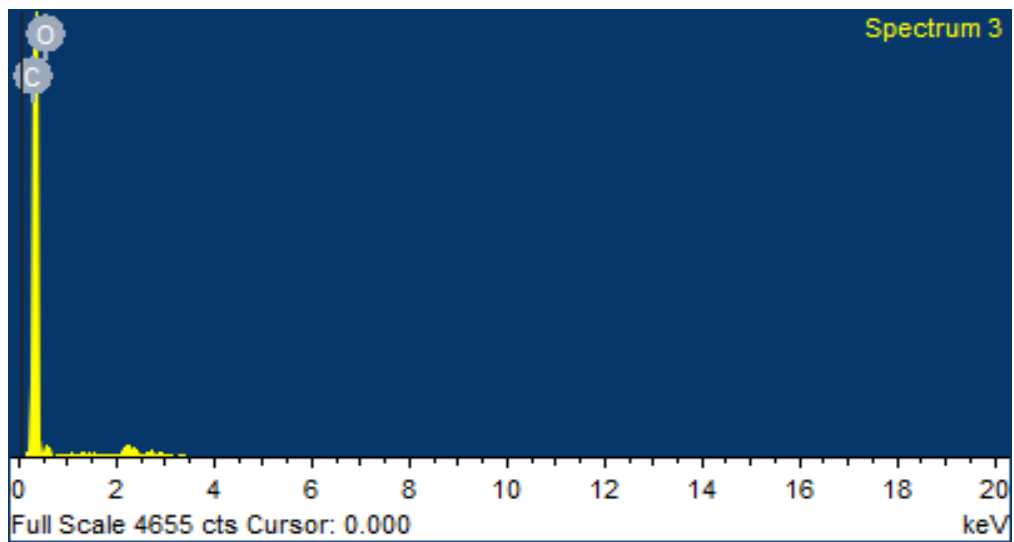

Fig 4.3 EDX Spectrum of ZnTe
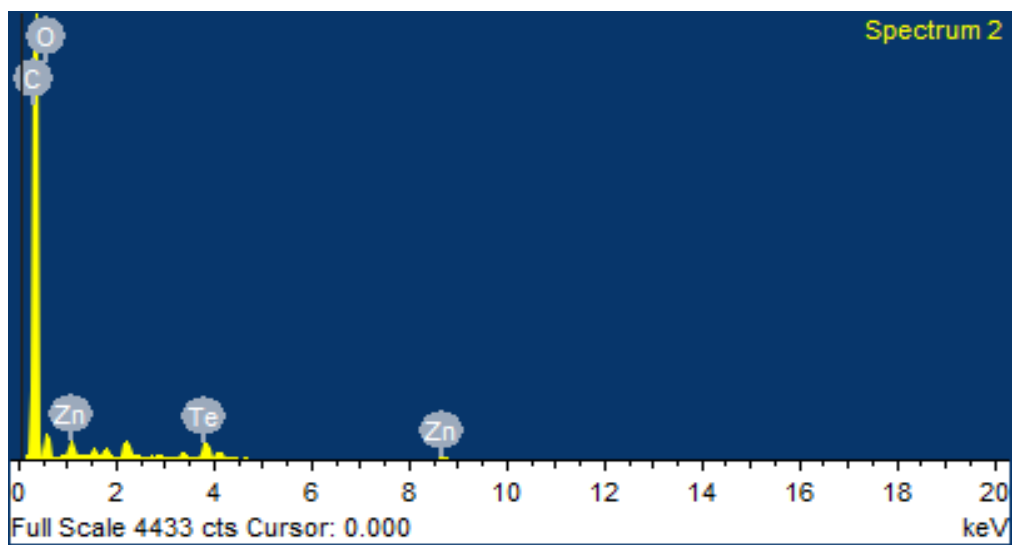
Fig 4.4 EDX Spectrum of N-RGO

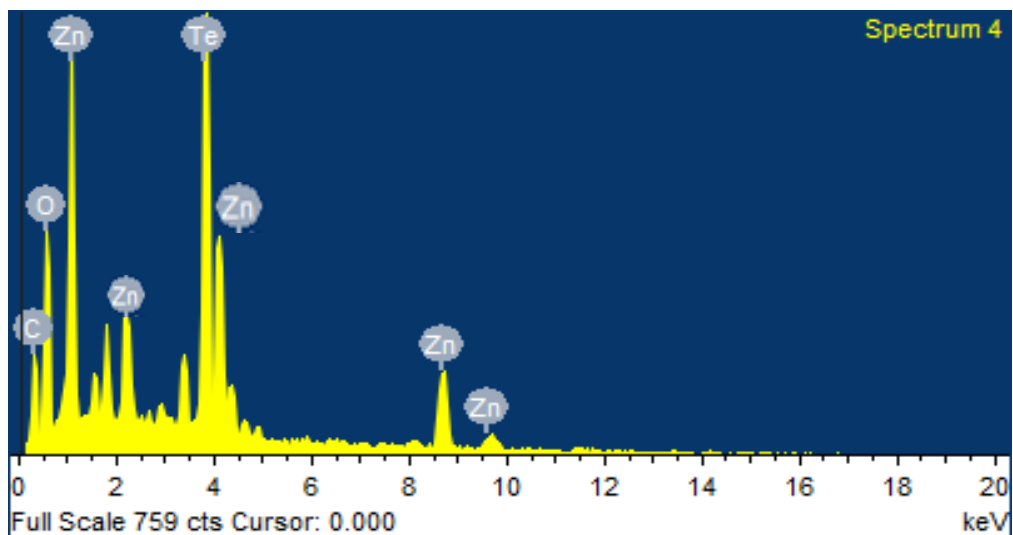**Fig 4.5 EDX Spectrum of 1:3 ZnTe-NRGO**
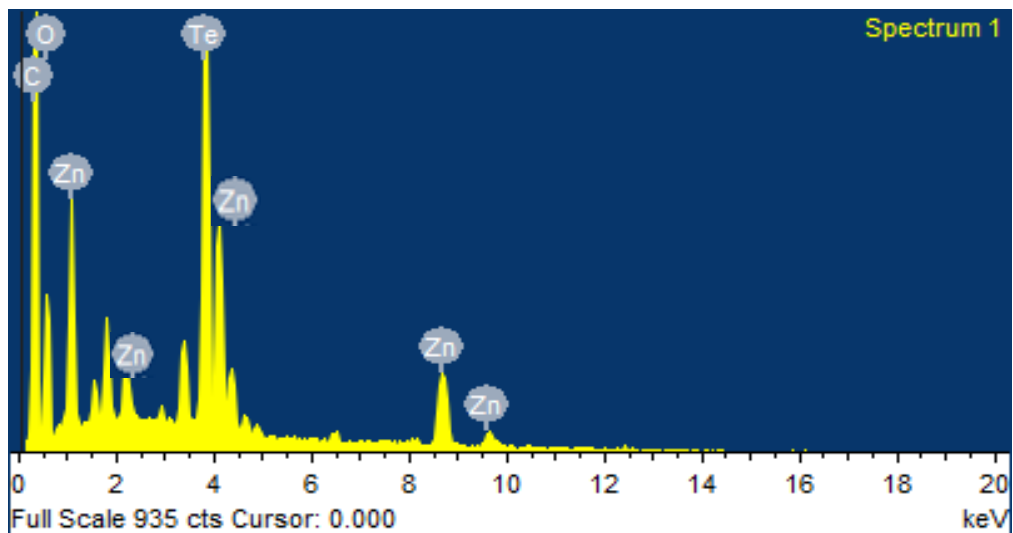
Fig 4.6 EDX Spectrum of 1:1 ZnTe-N-RGO

Fig 4.7 EDX Spectrum of 3:1 ZnTe-N-RGO

Table 4.1 Percentage composition of all elements in synthesized catalyst

Sample Code	Atomic % of Zn	Atomic % of Te	Atomic % of C	Atomic % of O
ZnTe	44.49	55.51	-	-
N-RGO	-	-	92.15	7.85
1:3 ZnTe-NRGO	0.21	0.28	87.75	11.77
1:1 ZnTe-NRGO	1.44	1.64	61	35.36
3:1ZnTe-NRGO	6.72	8.51	47.94	36.83

4.4 Alignment of Energy Levels:

Photo catalytic activity of all the prepared catalyst can be investigated through alignments of its energy level, which can be determined in terms of conduction and valence band position. XPS analysis was done to find the valence band position of zinc telluride. **Fig 4.8 (a)** shows the valence band position spectra of ZnTe .The zoom- in plots of the measured valence band position which is 0.47eV are shown in **fig 4.8 (b).**
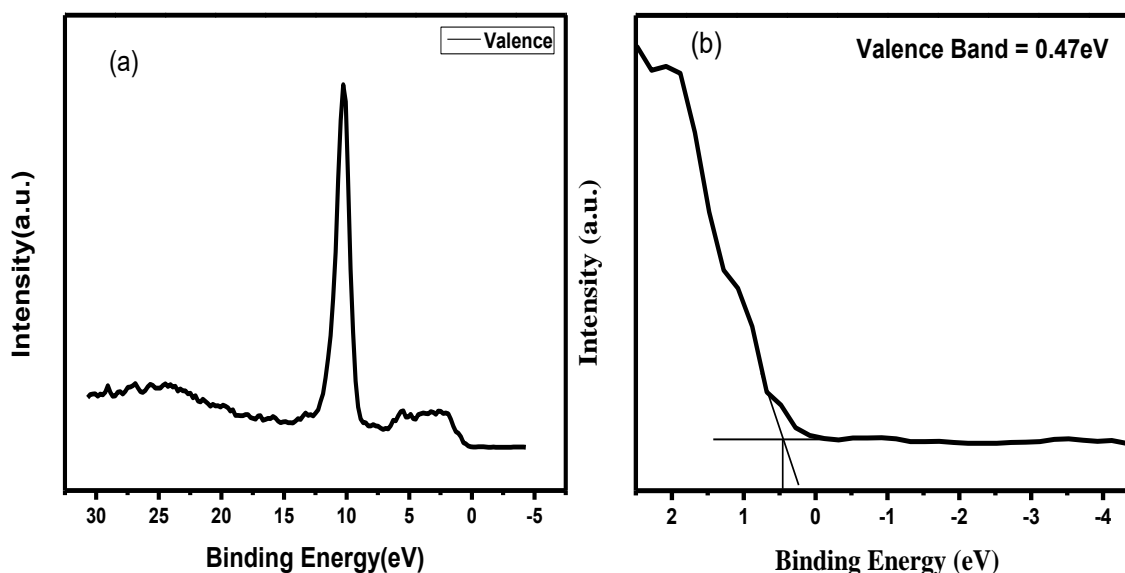

Fig.4.8: (a) XPS valence band Spectrum and (b) Zoom in valence band edge of ZnTe

UV-Vis/DRS was used to examine the band gap and optical properties of prepared catalysts.DRS measure the reflectance factor instead of absorption factor. The band gap value of catalysts is calculated via tauc plot, obtain by plotting $(\alpha h\nu)^2$ on y-axis and $(h\nu)$ on x-axis [7]

$$(\alpha h\nu)^2 = K\,(h\nu - Eg)$$

Where α is the absorption coefficient, K is the proportionality constant and v is the frequency of photons.To measure the absorption coefficient Kubelka-Munk expression is used. Based on the DRS results, the band edge positions of the catalysts were calculated theoretically using the Mulliken electronegativity theory following the empirical formula

$$E_{VB} = x - E^e + 0.5E_g \tag{1}$$

$$E_{CB} = E_{VB} - E_g \tag{2}$$

Where E_{VB}, E_{CB} and E_g are the valence band edge potential, conduction band edge potential, band gap of the semiconductor, respectively. The term E^e is the scale factor of the hydrogen reference electrode and x is the absolute electronegativity of the semiconductor [8].**Fig 4.9(a)** represents absorption spectrum of zinc telluride which clearly shows the strong absorption peak in green area of visible light at approximately 559nm.The band gap value of ZnTe calculated via tauc plot was found to be 2.2eV (insect of **Fig. 4.9**) [9].The UV-vis absorption spectrum of NRGO exhibited absorption peak at 735nm and the optical band gap value calculated through tauc plot was determined to be 1.7eV [10] as shown in the insect of **fig 4.10.**
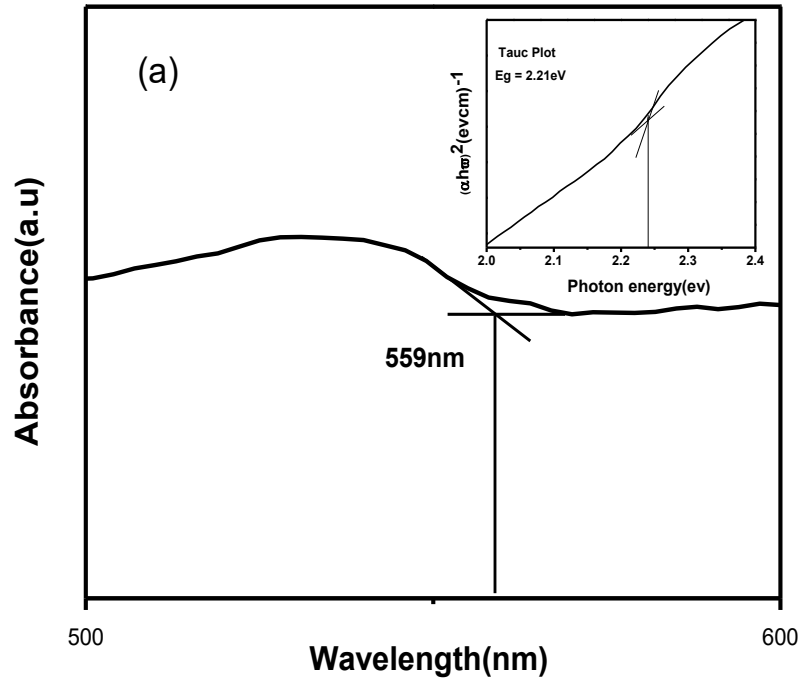
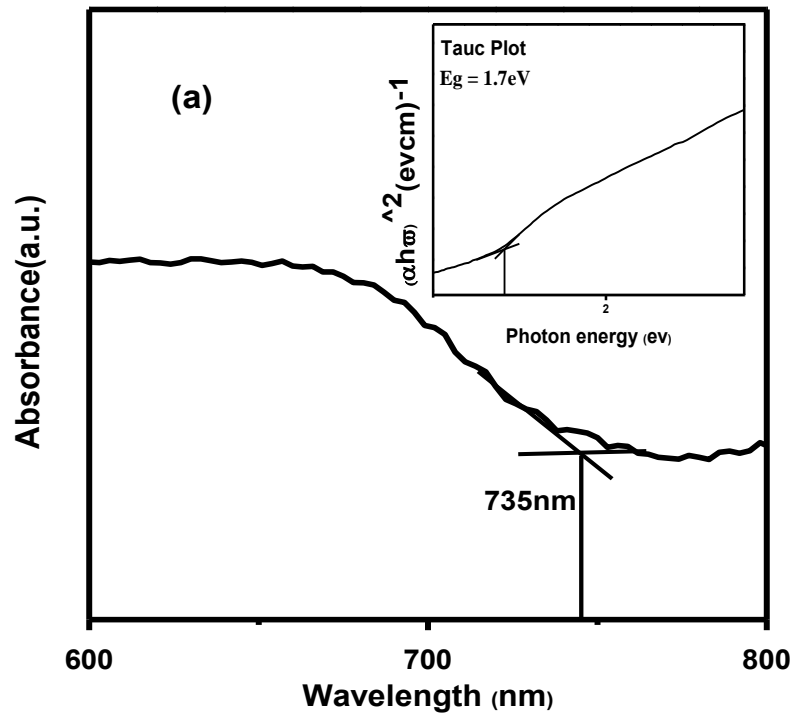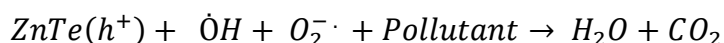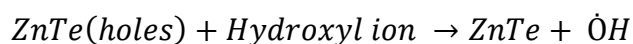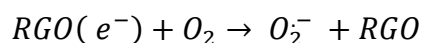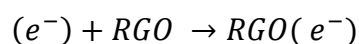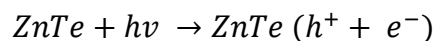**Figure 4.9: UV/vis diffuse reflectance spectrum and tauc plot for ZnTe**

Figure 4.10: UV/vis diffuse reflectance spectrum and tauc plot for N-RGO

On the basis of experimental facts, a cautious mechanism for the photodegradation of dyes on ZnTe/N-RGO nanocomposites have been suggested that is shown in **scheme 8.** This scheme shows that when light fall on surface of photocatalst the e⁻s from VB get excited to the CB of zinc telluride producing e⁻ and h⁺ pairs. NRGO incorporated to the zinc telluride works as electron accumulator and carrier, as a result separation efficiency of charge carriers' rises that sequentially enhances the life time of charge carrier and also increase the interfacial charge transferred efficiency from the zinc telluride to the NRGO thus increasing the photocatalytic activity. The electropositive holes produced at valence band are accountable for the production of (OH·) radical. The photogenrated CB e⁻s hence moved from the bulk of ZnTe react with dissolved oxygen molecules to formed superoxide radical ion ($O_2^{-·}$).Because of high transportation ability and large surface area of N-graphene the as generated super oxide and hydroxyl radical ions move from the solution of catalyst to the surface and break down the pollutants into carbon dioxide, water and mineral salts.
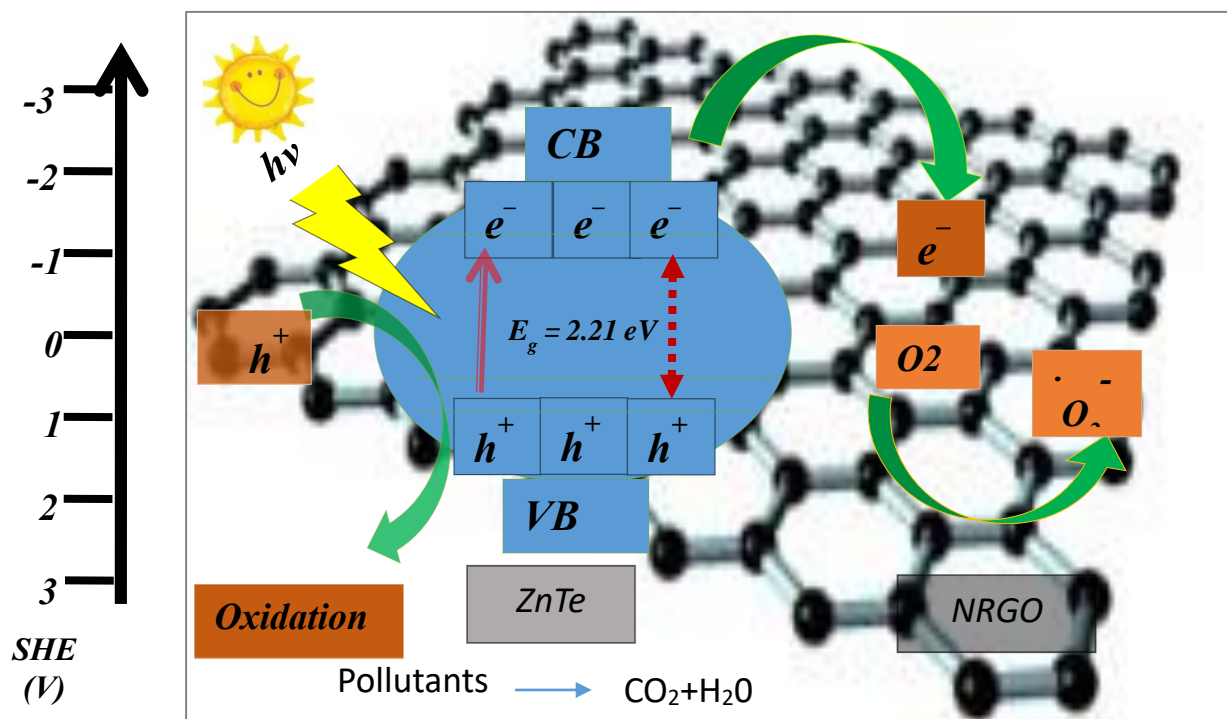
Scheme 8: Photocatalytic mechanism for degradation of dye over ZnTe-NRGO

The probable mechanism of photodegradation is assumed below:

$$ZnTe + hv \rightarrow ZnTe\ (h^+ +\ e^-)$$

$$(e^-) + RGO \rightarrow RGO(\ e^-)$$

$$RGO(\ e^-) + O_2 \rightarrow O_2^- + RGO$$

$$ZnTe(holes) + Hydroxyl\ ion \rightarrow ZnTe + \dot{O}H$$

$$ZnTe(h^+) + \ \dot{O}H + \ O_2^{-\cdot} + Pollutant \rightarrow H_2O + CO_2$$

4.5: Degradation Studies:

Finally, all the synthesized photocatalyst were used for degradation of CR dye in visible light radiation and consequences are displayed in **fig 4.12.** The formula used for the calculation of degradation efficacy of CR dye is given below;

Degradation efficiency = [(Co-Ct) / Co x 100]

Where Co is the concentration of dye at time 0 and Ct is the concentration of CR dye at time t.

Results shows that pure N-RGO has greater photocatalytic activity towards CR degradation, up to 78% as compared to pure ZnTe. This can be attributed to smaller band gap value (1.7eV) of NRGO, which allow the formation of large number of carriers under visible light irradiation, degrading the molecules of CR dye. However, the ZnTe-NRGO nanocomposites were show high photocatalytic efficiency, with 97.6%, 81.6% and 79.2% of CR photo degraded for 1:1 ZnTe NRGO, 1:3 ZnTe-NRGO and 3:1 ZnTe-NRGO respectively. The improvement in the photocatalytic activity of the ZnTe/NRGO nanocomposites could be credited to the NRGO that act as good e⁻ acceptor and carrier as a result it decreases the charge recombination rate by increasing charge separation.

- Among all nanocomposites, 1:1 ZnTe-NRGO photacatalyst exhibited highest photocatalytic activity towards Congo red dye because of equal ratio of ZnTe and NRGO. But as the amount of N-doped reduced graphene oxide during composite formation increases or decreases from the optimum level, the photocatalytic activity is affected. This is because at higher N-graphene content, graphene sheet

68

clenched together and forms multilayer sheets which lead to the shielding of active sites on the surface of catalysts. The shielding leads to the dispersion of photons and hence reduces light absorption of photocatalyst, lowering excitation efficiency of zinc telluride [7].

- Another factor which is considered important in determining the photocatalytic degradation process is surface morphology like agglomerate size and particle size as there is direct connection between surface coverage of photocatalyst and organic compounds [11]. In 1:1 ZnTe-NRGO the nanoparticles are well decorated on the surface of N-graphene sheet, more active sites are available which increases the adsorption of dyes and results into higher photocatalytic efficiency i.e. 97.6% as compared to 1:3 ZnTe-NRGO and 3:1 ZnTe-NRGO in which large agglomerates of nanoparticles are seen which is shown in section 4.2.
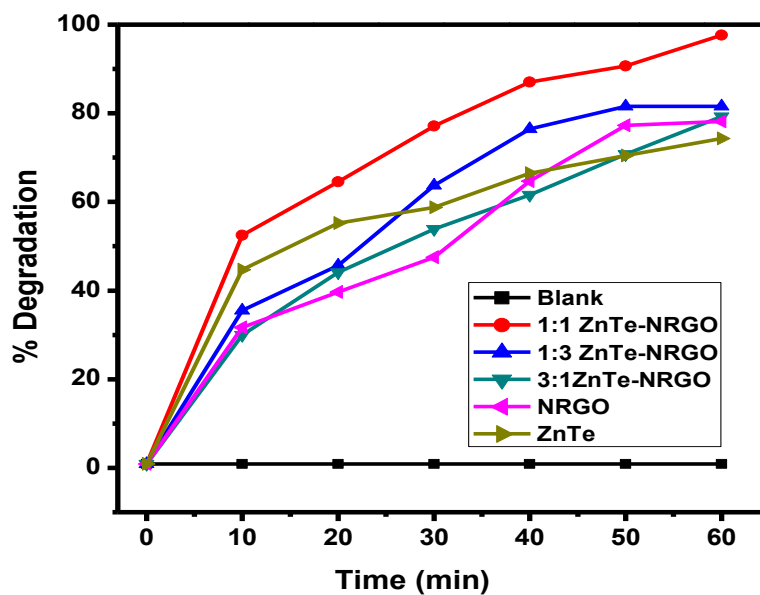

Figure 4.11: Activity of all the prepared sample against Congo red dye

This **table 4.2** summarizes the results of degradation of Congo red over ZnTe-NRGO photocatalyst.

Time (min)	10	20	30	40	50	60
Catalyst	**% Degradation of Congo Red Dye**					
ZnTe	44.70	55.18	58.75	66.44	70.4	74.3
NRGO	31.7	39.7	47.49	64.7	77.25	78.14
1:1ZnTe-NRGO	52.5	64.54	77.14	87.06	90.7	97.6
1:3ZnTe-NRGO	37.56	45.7	63.76	76.47	81.6	81.6
3:1ZnTe-NRGO	29.98	44.14	53.9	61.6	70.79	79.26

Table 4.2: Percentage of dye degraded with time using all the prepared catalyst

References:

[1]. Mi, Qian, Daiquan Chen, Juncheng Hu and Jinlin Li. "Nitrogen-doped graphene/CdS hollow spheres nanocomposite with enhanced photocatalytic performance." *Chinese Journal of Catalysis* 34.11 (2013): 2138-2145.

[2]. Derattrakul, Varisara, Wanwisa Limphirat, and Paisan Kongkachuichay. "Influence of reduction time of catalyst on methanol synthesis via CO_2 hydrogenation using Cu–Zn/N-rGO investigated by in situ XANES." *Journal of the Taiwan Institute of Chemical Engineers* 80 (2017): 495-502.

[3]. Sadiq, M. Mohamed Jaffer, U. Sandhya Shenoy, and D. Krishna Bhat. "$NiWO_4$-ZnO-NRGO ternary nanocomposite as an efficient photocatalyst for degradation of methylene blue and reduction of 4-nitro phenol." *Journal of Physics and Chemistry of Solids* 109 (2017): 124-133

[4]. Mi, Qian, Daiquan Chen, Juncheng Hu and Zhengxi Huang. "Nitrogen-doped graphene/CdS hollow spheres nanocomposite with enhanced photocatalytic performance." *Chinese Journal of Catalysis* 34.11 (2013): 2138-2145.

[5]. Lu, Zhen-Jiang, Mao-Wen Xu, Shu-Juan Bao and Kehfarn Tan. "Facile preparation of nitrogen-doped reduced graphene oxide as a metal-free catalyst for oxygen reduction reaction." *Journal of Materials Science* 48.23 (2013): 8101-8107.

[6]. Appavu, Brindha, Sivakumar Thiripuranthagan and Sudhakar. "$BiVO_4$/N-rGO nano composites as highly efficient visible active photocatalyst for the degradation of dyes and antibiotics in eco system." *Ecotoxicology and Environmental Safety* 151 (2018): 118-126.

[7]. Wen, Marilyn Yuen Sok, Abdul Halim Abdullah, and Lim Hong Ngee. "Synthesis of ZnO/rGO nanohybrid for improved photoctalytic activity." *Malaysian Journal of Analytical Sciences* 21.4 (2017): 889-900.

[8]. Sadiq, M. Mohamed Jaffer, U. Sandhya Shenoy, and D. Krishna Bhat. "Enhanced photocatalytic performance of N-doped RGO-$FeWO_4$/Fe3O4 ternary nanocomposite in environmental applications." *Materials Today Chemistry* 4 (2017): 133-141

[9]. Wang, Hai-Xia, Rong Wu, Shun-Hang Wei and Li-Rui Yu. "One-pot solvothermal synthesis of ZnTe/RGO nanocomposites and enhanced visible-light photocatalysis." *Chinese Chemical Letters* 27.9 (2016): 1572-1576

[10]. Seo, Sohyeon, Yeoheung Yoon, Junghyun Lee, Younghun Park, and Hyoyoung Lee "Nitrogen-doped partially reduced graphene oxide rewritable nonvolatile memory." *ACS Nanomaterial* 7.4 (2013): 3607-3615.

[11]. Kumar, A., and G. Pandey. "A review on the factors affecting the photocatalytic degradation of hazardous materials." *Material Science and Engineering* 1.3 (2017): 10018.

.

Summary and Future Prospects

In this thesis photocatalytic activity of effectively synthesized zinc telluride based nanocomposite photocatalysts has been checked by the degradation of Congo red dye. Zinc telluride as single photocatalyst meet some problems like fast electron hole recombination hence less photocatalytic activity. Nanocomposites formation approach with nitrogen doped reduced graphene oxide has been used to increase the efficacy of zinc telluride. Conclusion of complete work carried out is briefed as follow;

5.1 Conclusions:

- ZnTe and N-doped reduce graphene oxide has been successfully synthesized via hydrothermal method. Ammonia and hydrazine hydrate were used as a doping and reducing agent respectively in synthesis of N-doped RGO.
- Graphene oxides are also successfully synthesized through Hummer's method, which involved the oxidation of graphite using strong oxidizing agent $KMnO_4$.
- Nanocompoistes are synthesized from as-synthesized zinc telluride and nitrogen doped reduced graphene oxide via physical method in three different ratio that is 1:3ZnTe-NRGO, 1:1ZnTe-NRGO and 3:1 ZnTe-NRGO.
- The elemental composition, optical properties, phase structure and surface morphology of all prepared photocatalyst were observed by different methods.
- The visible light photocatalytic activities were studies in degradation of Congo red dye.
- Among all the photocatalyst 1:1ZnTe-NRGO showed highest photo degradation efficiency of 97.6% towards Congo red dye.
- The enhanced photocatalytic activity of all nanocomposites is credited to existence of NRGO, serve as e^- transporter and collector, which increased the transfer of photo generated electrons from CB of ZnTe to N-RGO sheet, thus decreasing the electron hole recombination, consequently increasing charge separation.

5.2 Future Outlooks:

To deal with current problems connected to environment and energy various strategies are developed. One of the favorable approaches for waste water treatment is photodegradation of dyes, producing water pollution by photocatalysis.Consideration should be paid to some of the following different issues in future:

- Use of all the synthesized nanocomposites for different other applications like for reduction of carbon dioxide and for water splitting.
- Also all the synthesized catalysts will be used for degradation of other dyes, antibiotics and pesticides and their activity will be measured.
- XPS analysis will be carried out to find the surface chemical composition of NRGO and to determine the optimum level of nitrogen for doping of graphene.
- Effective approach must be developed to facilitate the electron hole separation that is the important steps towards synthesis of photocatalysts.
- GC-MS analysis will be carried out to study the degradation mechanism of CR and type of intermediate products produced in photocatalytic degradation of Congo red dye